The Plant Cell, Vol. 29: 1907–1926, August 2017, www.plantcell.org © 2017 ASPB.

SG2-Type R2R3-MYB Transcription Factor MYB15 Controls Defense-Induced Lignification and Basal Immunity in Arabidopsis

William R. Chezem,[a] Altamash Memon,[a] Fu-Shuang Li,[b] Jing-Ke Weng,[b,c] and Nicole K. Clay[a,1]

[a] Department of Molecular, Cellular, and Developmental Biology, Yale University, New Haven, Connecticut 06511
[b] Whitehead Institute for Biomedical Research, Cambridge, Massachusetts 02142
[c] Department of Biology, Massachusetts Institute of Technology, Cambridge, Massachusetts 02139

ORCID IDs: 0000-0003-3059-0075 (J.-K.W.); 0000-0002-9531-9932 (N.K.C.)

Lignification of cell wall appositions is a conserved basal defense mechanism in the plant innate immune response. However, the genetic pathway controlling defense-induced lignification remains unknown. Here, we demonstrate the *Arabidopsis thaliana* SG2-type R2R3-MYB transcription factor MYB15 as a regulator of defense-induced lignification and basal immunity. Loss of MYB15 reduces the content but not the composition of defense-induced lignin, whereas constitutive expression of *MYB15* increases lignin content independently of immune activation. Comparative transcriptional and metabolomics analyses implicate *MYB15* as necessary for the defense-induced synthesis of guaiacyl lignin and the basal synthesis of the coumarin metabolite scopoletin. MYB15 directly binds to the secondary wall MYB-responsive element consensus sequence, which encompasses the AC elements, to drive lignification. The *myb15* and lignin biosynthetic mutants show increased susceptibility to the bacterial pathogen *Pseudomonas syringae*, consistent with defense-induced lignin having a major role in basal immunity. A scopoletin biosynthetic mutant also shows increased susceptibility independently of immune activation, consistent with a role in preformed defense. Our results support a role for phenylalanine-derived small molecules in preformed and inducible Arabidopsis defense, a role previously dominated by tryptophan-derived small molecules. Understanding the regulatory network linking lignin biosynthesis to plant growth and defense will help lignin engineering efforts to improve the production of biofuels and aromatic industrial products as well as increase disease resistance in energy and agricultural crops.

INTRODUCTION

Lignin is essential for the structural integrity of the vascular cell wall, providing mechanical support for plants to stand upright and serving as a scaffold for long-distance water transport (Boerjan et al., 2003); its role in vascular cell wall development may have allowed land plants to dominate the terrestrial ecosystem (Weng and Chapple, 2010). Lignin is also one of the most difficult biopolymers to degrade due to the nature and heterogeneity of its linkages (Vanholme et al., 2010). Unfortunately, lignin makes plant cell walls recalcitrant to conversion to fermentable sugars and cellulose fibers for bioenergy uses and pulp/paper production, respectively (Chen and Dixon, 2007; Dien et al., 2009; Novaes et al., 2010). Because of its significant economic impact, lignin biosynthesis is one of the most intensively studied subjects in plant biochemistry, resulting in genetic, -omics, and systems-level characterizations of the monolignol biosynthetic pathway in *Arabidopsis thaliana* (Bonawitz and Chapple, 2010; Vanholme et al., 2012), switchgrass (*Panicum virgatum*; Shen et al., 2013), and poplar (*Populus trichocarpa*; Shuford et al., 2012; Chen et al., 2014).

Lignin may have also functioned as a defensive chemical barrier against biotrophic pathogens in the first vascular plants (Raven, 1984). Defense-induced lignification is a conserved basal defense mechanism in the plant immune response against (hemi)-biotrophic pathogens in a wide range of plant species (Vance, 1980; Nicholson and Hammerschmidt, 1992; Siegrist et al., 1994; Lange et al., 1995; Baayen et al., 1996; Smit and Dubery, 1997; Menden et al., 2007; Bhuiyan et al., 2009) and has been used as a biochemical marker of an activated immune response for decades (Ride, 1975; Vance, 1980; Lawton and Lamb, 1987; Robertsen, 1986; Lesney, 1989; Kishi-Kaboshi et al., 2010; Adams-Phillips et al., 2010). Efforts to manipulate lignin content and composition have primarily focused on the eleven enzymatic steps of the monolignol biosynthetic pathway (Supplemental Figure 1) (Boerjan et al., 2003; Li et al., 2008; Sattler et al., 2010; Vanholme et al., 2013), in which monolignols are synthesized from the amino acid L-phenylalanine, and then oxidatively polymerized into *p*-hydroxyphenyl (H), guaiacyl (G), or syringl (S) units. While genetic alterations in the monolignol pathway can impact plant defense and growth, they do not distinguish between vascular cell wall lignification and defense-induced lignification. Thus, it remains unclear whether defense-induced lignification plays a significant role in plant immunity, and if so, which component of defense-induced lignin is important for successful defense against (hemi)biotrophic pathogens.

[1] Address correspondence to nicole.clay@yale.edu.
The author responsible for distribution of materials integral to the findings presented in this article in accordance with the policy described in the Instructions for Authors (www.plantcell.org) is: Nicole K. Clay (nicole.clay@yale.edu).
www.plantcell.org/cgi/doi/10.1105/tpc.16.00954

Plants have a multitiered pathogen recognition system. The first layer involves the cell surface perception of conserved microbial components (i.e., pathogen-/microbe-associated molecular patterns [MAMPs]) and pathogen-generated plant signal molecules (damage-associated molecular patterns) by pattern recognition receptors and the subsequent activation of pattern-triggered immunity or basal immunity (Boller and Felix, 2009; Zipfel, 2014). The second layer involves the perception of race-specific pathogen effectors on the cell surface and in the cytosol by resistance (R) proteins and the subsequent activation of effector-triggered immunity or R-mediated immunity (Jones and Dangl, 2006). More importantly, the microbial elicitation of basal or R-mediated immunity has been shown to activate the biosynthesis and deposition of lignin in cell wall appositions (Robertsen, 1986; Lesney, 1989; Lee et al., 2001; Kishi-Kaboshi et al., 2010; Adams-Phillips et al., 2010).

The monolignol pathway contributes to local resistance to (hemi)biotrophic pathogens. For example, in wheat (*Triticum aestivum*), transient downregulation of monolignol pathway enzymes phenylalanine ammonia-lyase (PAL), caffeoyl-CoA *O*-methyltransferase (CCoAOMT), caffeic acid *O*-methyltransferase (COMT), and cinnamyl alcohol dehydrogenase (CAD), individually and pairwise, by RNAi-mediated gene silencing led to decreased basal immunity or penetration resistance to the virulent and nonhost biotrophic fungal pathogens *Blumeria graminis* f. sp *tritici* and *Blumeria graminis* f. sp *hordei*, respectively (Bhuiyan et al., 2009). In addition, specific inhibition of the monolignol pathway enzyme cinnamoyl-CoA reductase (CCR) led to repressed R-mediated immunity to the biotrophic fungal pathogen *Puccinia graminis* (Moerschbacher et al., 1990). In rice (Oryza sativa), CCR may also contribute to R-mediated immunity against the hemibiotrophic fungal pathogen *Magnaporthe grisea* (Kawasaki et al., 2006; Ono et al., 2001). In Arabidopsis and tobacco (*Nicotiana tabacum*), loss or downregulation of PAL led to decreased basal immunity to the hemibiotrophic bacterial pathogen *Pseudomonas syringae* (Huang et al., 2010) and to the biotrophic viral pathogen tobacco mosaic virus (Elkind et al., 1990; Pallas et al., 1996), respectively. Because PAL is also involved in biosynthesis of the defense signal molecule salicylic acid (SA), which mediates local and systemic resistance to many (hemi)biotrophic pathogens (Sticher et al., 1997), it remains unclear whether the reduced resistance in PAL-deficient plants is due to significant reductions in lignin, SA, or both.

The lignin polymer in angiosperm plants is typically composed of G- and S-units with low to trace amounts of H units, whereas the lignin from nonflowering vascular plants is mostly composed of G units with minor amounts of H units (Vanholme et al., 2010). The ratio of S- to G-units in lignin indicates the degree and nature of polymeric cross-linking. S-rich lignin is less condensed, linked by more labile ether bonds at the 4-hydroxyl position (Ferrer et al., 2008), and thus more amenable to degradation. In contrast, G-rich lignin is more cross-linked due to a greater proportion of biphenyl and other carbon-carbon bonds and thus is more recalcitrant to depolymerization than S-rich lignin. G-rich lignin should be a better defensive barrier against pathogens but increases in G-lignin content in Arabidopsis through genetic manipulation of the monolignol pathway has led to a reduction, not increase, in R-mediated immunity to the hemibiotrophic bacterial pathogen *P. syringae* (Goujon et al., 2003; Quentin et al., 2009). Thus, the role of G-rich lignin in basal immunity remains unknown. Defense-induced lignin appears to have increased levels of H-units compared with lignin found in vascular cell walls (Ride, 1975; Hammerschmidt et al., 1985; Doster and Bostock, 1988; Robertsen and Svalheim, 1990; Lange et al., 1995), but the functional relevance for this is not known.

Recently, transcription factors have been used to manipulate lignin content and composition of vascular cell walls in a variety of plant species (Li et al., 2008; Sattler et al., 2010; Zhou et al., 2009; Zhong and Ye, 2009; Scully et al., 2016). In Arabidopsis, at least four subfamilies of R2R3-MYB transcription factors have been shown to transactivate the promoters of monolignol pathway genes, including MYB85, the SG3-type R2R3-MYBs MYB58 and MYB63, the SG13-type R2R3-MYBs MYB46 and MYB83, and related MYBs MYB20, MYB42, and MYB43 (Newman et al., 2004; Zhong et al., 2007, 2008; McCarthy et al., 2009: Zhou et al., 2009). Of these, only the SG3-type R2R3-MYBs MYB58 and MYB63 have been shown to directly activate nearly all of the genes in the monolignol pathway (Zhou et al., 2009). Overexpression of *MYB58* or its co-ortholog *MYB63* specifically activated the monolignol pathway and lignin accumulation at the expense of biomass production (Zhou et al., 2009). Conversely, dominant repression of their functions reduced lignin content at the expense of upright inflorescence development (Zhou et al., 2009). While the role of SG3-type R2R3-MYBs in vascular cell wall lignification appears to be conserved in dicot plants (Zhong and Ye, 2009), their role in lignification in monocots appears unclear. MYB58/63 orthologs in sorghum (*Sorghum bicolor*) and maize (*Zea mays*; e.g., SbMYB60 and ZmMYB19/Zm1) induced marginal increases in lignin content (Scully et al., 2016) and reduced metabolic flux to the monolignol pathway by activating the rival flavonoid biosynthetic pathway (Franken et al., 1994). In addition, it is not known whether MYB58/63 can regulate defense-induced lignification in Arabidopsis or whether another gene pathway not yet described controls defense-induced lignification in Arabidopsis and other plant species.

The transcriptional regulation of lignification is a topic of great interest because of its potential utility in developing low- or high-lignin biomass feedstocks and disease-resistant crops. Here, we show the SG2-type R2R3-MYB transcription factor MYB15 as a novel regulator of inducible and preformed plant defense. MYB15 is required for the defense-induced synthesis of G-rich lignin and the constitutive synthesis of the coumarin metabolite scopoletin, both of which contribute to disease resistance against a hemibiotrophic bacterial pathogen.

RESULTS

MYB15 Is Necessary for Defense-Induced Lignification

Basal immunity has been shown to transcriptionally activate the monolignol biosynthetic pathway in different plant species (Lawton and Lamb, 1987; Kaku et al., 2006; Zipfel et al., 2006; Denoux et al., 2008). To identify transcriptional regulators involved in defense-induced lignification, we used the MAMP elicitor flg22—the bioactive epitope of bacterial flagellin (Gómez-Gómez and Boller, 2000)—to transcriptionally activate the monolignol

pathway in Arabidopsis seedlings under the same conditions as a previous transcriptomic profiling study (Denoux et al., 2008). We then screened a collection of Arabidopsis mutants defective in flg22-inducible transcription factors (Clay et al., 2009) using phloroglucinol-HCl staining, which specifically detects coniferaldehyde end groups of G-lignin units (Clifford, 1974). Consistent with a previous study (Adams-Phillips et al., 2010), flg22 induces uniform staining of cotyledons in wild-type plants but not in the *fls2* mutant (Figure 1A), which lacks the functional flg22 receptor (Gómez-Gómez and Boller, 2002). These results indicate that the observed lignification is a consequence of flg22 perception. We identified two loss-of-function T-DNA insertion mutants of *MYB15*, *myb15-1* and *myb15-2* (Figure 1B), that are impaired in the flg22-induced lignin response (Figure 1A). Consistent with a previous study (Adams-Phillips et al., 2010), the MAMP elicitor elf26, a bioactive epitope of bacterial EF-*Tu* (Kunze et al., 2004), also induces lignification in wild-type plants but not in the *efr* mutant (Supplemental Figure 2A), which lacks the functional elf26 receptor (Zipfel et al., 2006). *MYB15* is not only transcriptionally upregulated in response to elf26 (Zipfel et al., 2006), but the *myb15* mutants are also impaired in the elf26-induced lignin response (Supplemental Figure 2A), demonstrating a conserved requirement for MYB15 in lignification associated with basal immunity. In addition to flg22 and elf26, *MYB15* is reportedly upregulated 2.5-fold in response to the bacterial MAMP elicitor harpinN_{EA} (Liu et al., 2010).

To investigate whether *MYB15* is sufficient to induce lignification, we used the two-component glucocorticoid-inducible system (Aoyama and Chua, 1997; McNellis et al., 1998) to generate *myb15-1* mutant plants that in the presence of the glucocorticoid hormone dexamethasone (Dex) express a wild-type copy of the *MYB15* gene with a C-terminal fusion to *6x c-Myc* (*DEX:MYB15-myc*). In addition, we used the *CaMV35S* promoter to generate *myb15-1* mutant plants that constitutively express the wild-type *MYB15* gene (*35S:MYB15*). Both induced and constitutive expression of *MYB15* restored the flg22-induced lignin response in the *myb15-1* mutant to wild-type levels (Figure 1D; Supplemental Figure 2A).

MYB15 is an SG2-type R2R3-MYB transcription factor, containing a pair of highly conserved SG2 motifs in its C-terminal region (Stracke et al., 2001) (Figure 1B; Supplemental Figure 3). It is reportedly expressed constitutively at low levels during both vegetative and reproductive growths (Ding et al., 2009). Phylogenetic analysis and sequence alignment indicate MYB15 is closely related to the SG3-type R2R3-MYB transcription factors MYB58 and MYB63 (Supplemental Figures 3 and 4), which are involved in vascular cell wall lignification (Zhou et al., 2009). While *MYB15* is transcriptionally upregulated in response to flg22, *MYB58* and *MYB63* are transcriptionally repressed or largely unchanged, respectively, in a MYB15-independent manner (Figure 1C). To confirm that SG3-type R2R3-MYBs do not regulate defense-induced lignification, we isolated T-DNA insertion mutants of *MYB58* and *MYB63* (Supplemental Figure 5A) and observed that the single mutants *myb58* and *myb63* and the double mutant *myb58/63* are not impaired in the flg22-induced lignin response (Figure 1A). These results indicate that MYB15 mediates defense-induced lignification independently of MYB58/63.

Defense-Induced Lignification Contributes to Plant Growth

Perturbations in lignin biosynthesis often affect inflorescence growth. For example, the inflorescence stems of monolignol pathway mutants *cse-2* and *ccr1-6* reportedly are 37% and 34% shorter, respectively, than the wild type, when grown under short-day to long-day conditions (Van Acker et al., 2013; Vanholme et al., 2013). To investigate whether perturbations in the regulation of lignin biosynthesis also affect plant growth, we compared the inflorescence stem heights of SG2- and SG3-type R2R3-MYB transcription factor mutants with those of the wild type and monolignol pathway mutants when grown under day-neutral to long-day conditions. While the *myb58* and *myb63* mutants have slightly reduced inflorescence growths (4.6% shorter than the wild type) (Supplemental Figure 5A), the *myb58/63* double mutant is comparable to the monolignol pathway mutant *cse-2* (23.1 and 28.3% shorter than the wild type, respectively) (Supplemental Figure 5A). Similarly, the *myb15-1* and *myb15-2* mutants have slightly reduced inflorescence growths (from 11.1 to 13.3% shorter than the wild type) (Supplemental Figure 5A) and are comparable to the monolignol pathway mutants *pal1-3* and *ccr1-6* (16.7 and 13.9% shorter than the wild type, respectively) (Supplemental Figure 5B). These results suggest that vascular cell wall lignification and defense-induced lignification both contribute to plant growth.

MYB15 Is Sufficient for flg22-Induced Lignification

As phloroglucinol-HCl staining revealed qualitative difference in lignification between the wild type and *myb15* mutants, we further measured lignin content in whole seedlings using the acetyl bromide (AcBr) method (Moreira-Vilar et al., 2014). Mature wild-type (Col-0 ecotype) inflorescence stems reportedly contain 145 to 200 mg of AcBr lignin per gram of dry cell wall residue (g CWR) (Rohde et al., 2004; Van Acker et al., 2013). By contrast, 11-d-old wild-type seedlings contain 35.2 ± 4.34 mg lignin per g CWR (mean ± SD of four independent experiments) (Figures 2A to 2D), which is 4- to 5.7-fold less lignin than stem tissues containing fully lignified vascular cells. Consistent with our phloroglucinol-HCl staining results, flg22 treatment slightly but significantly increased the lignin content in wild-type plants (Figure 2A). Surprisingly, loss and gain of MYB15 function reduced and increased lignin content, respectively, independently of immune activation (Figures 2B to 2D). The phloroglucinol-HCl staining method appears not able to detect lignin accumulation in seedlings in the absence of flg22 elicitation and thus should not be used to qualitatively measure lignification in unelicited seedlings. These results suggest that MYB15 is sufficient to activate lignin biosynthesis.

Lignin monomer composition was evaluated by the derivatization followed by reductive cleavage (DFRC) method (Lu and Ralph, 1998), a procedure specific for β-*O*-4-linked lignin units. Lignin in wild-type stems is composed of 291.7 ± 152.8 μmol G-units and 175.2 ± 94.5 μmol S units per g CWR (mean ± SD; Vargas et al., 2016), with the S-unit content increasing from <6 to >26 mole percent during stem development (Meyer et al., 1998). By contrast, lignin in 11-d-old wild-type seedlings is composed of 0.69 ± 0.27 μmol G-units per g CWR (mean ± SD of

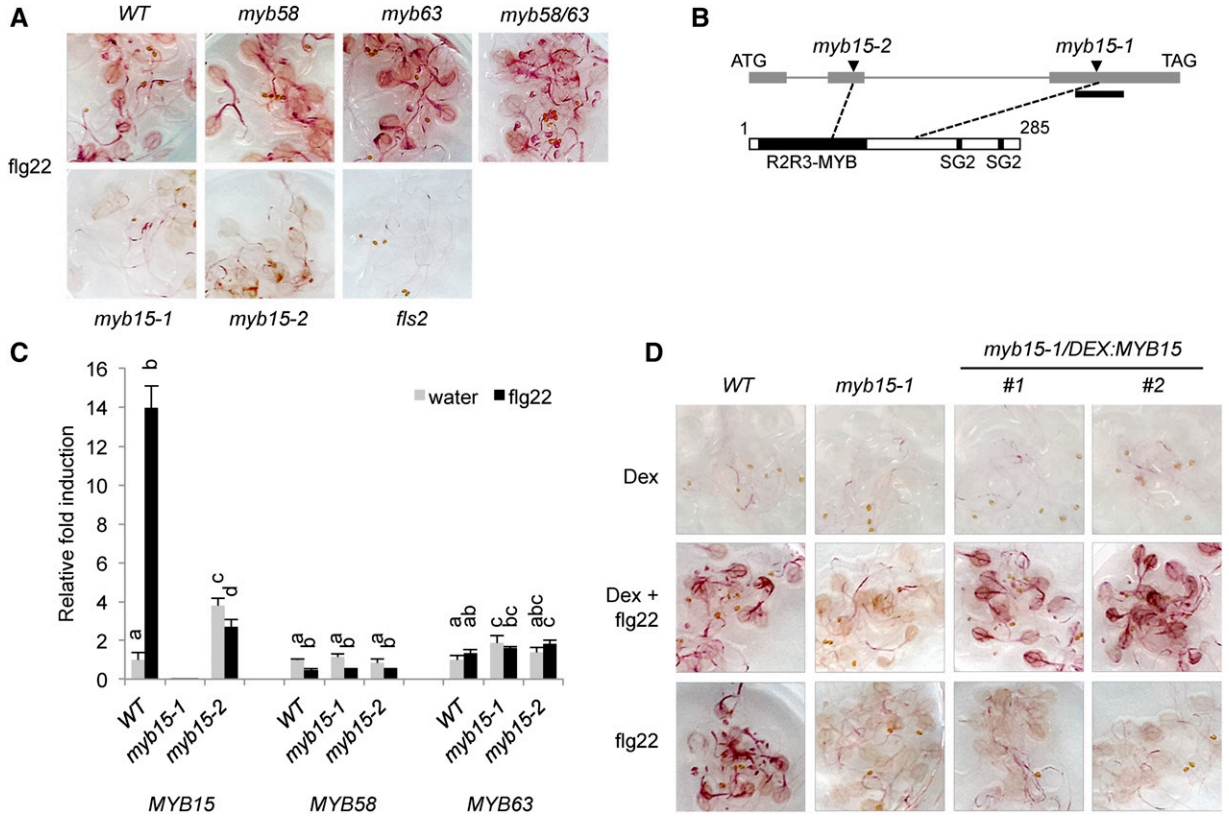

Figure 1. *MYB15* Is Required for Defense-Induced Lignification.

(A) Lignin analysis by phloroglucinol-HCl staining. Seven-day-old seedlings elicited with 1 μM flg22 for 48 h. Samples were stained at the same time, and intensity of purple-red staining correlates with lignin content.

(B) Schematic representation of the *MYB15* gene (top) and protein (bottom). Gray boxes indicate exons; triangles, positions of T-DNA insertions; thick black line, the corresponding transcript region amplified by qPCR in **(D)**; dashed lines, the corresponding T-DNA insertion sites.

(C) qPCR analysis of *MYB15*, *MYB58*, and *MYB63* transcripts in 9-d-old seedlings elicited with water or 1 μM flg22 for 3 h. Expression values are normalized to that of *eIF4A1* housekeeping gene and relative to those of water-treated wild-type sample. Data represent mean ± SD of four replicates of 10 to 15 seedlings each. Different letters denote statistically significant differences ($P < 0.05$, two-tailed *t* test).

(D) Lignin analysis of two independent *DEX:MYB15* lines by phloroglucinol-HCl staining. Seven-day-old seedlings elicited with 20 μM Dex and/or 1 μM flg22 for 72 h. Samples were stained at the same time.

two separate experiments) with trace amounts of S- and H-units detected in only some of the samples (Figures 2E and 2F). Consistent with our AcBr lignin results, flg22 treatment increased overall lignin content to >2.3 ± 0.03 μmol per g CWR (Figure 2E), with the S-unit content increasing to 26.7 mole percent (Figure 2F). Similarly, MYB15 overexpression increased overall lignin content to 1.17 ± 0.21 μmol per g CWR (Figure 2E), with the S-unit content increasing to 7 mole percent (Figure 2F). Consistent with the phloroglucinol-HCl staining results (Supplemental Figure 2D), the combination of flg22 treatment and *MYB15* overexpression additively increased overall lignin content to 7.21 ± 0.18 μmol of lignin per g CWR (Figure 2E), with the S-unit content increasing to 38.6 mole percent (Figure 2F). Together, these results lend further support to the sufficiency of MYB15 to activate lignification.

Upon flg22 elicitation, *myb15* mutants have reduced G- and S-lignin content compared with wild-type plants (Figure 2E), consistent with the AcBr lignin results in unelicited plants (Figures 2B and 2C). We could not confirm that the *myb15* mutants have reduced lignin content compared with wild-type plants in the absence of immune activation (Figure 2E), possibly for the reason that the low lignin amounts present in unelicited seedlings are near the limit of detection with this method.

MYB15 Activates Genes Involved in the Biosynthesis of G-Lignin, but Not S-Lignin

Our DFRC results indicate that defense-induced lignin in seedlings contains a greater percentage of S-units than vascular lignin (Figure 2F). However, the percentage of S-units in *myb15* mutants is unchanged upon immune activation compared with wild-type plants (Figure 2F), suggesting that MYB15 is not responsible for the mole percent increase in S-units in defense-induced lignin.

Lignin monomer composition is dictated by the expression of the monolignol pathway gene ferulate-5-hydroxylase (*F5H*)

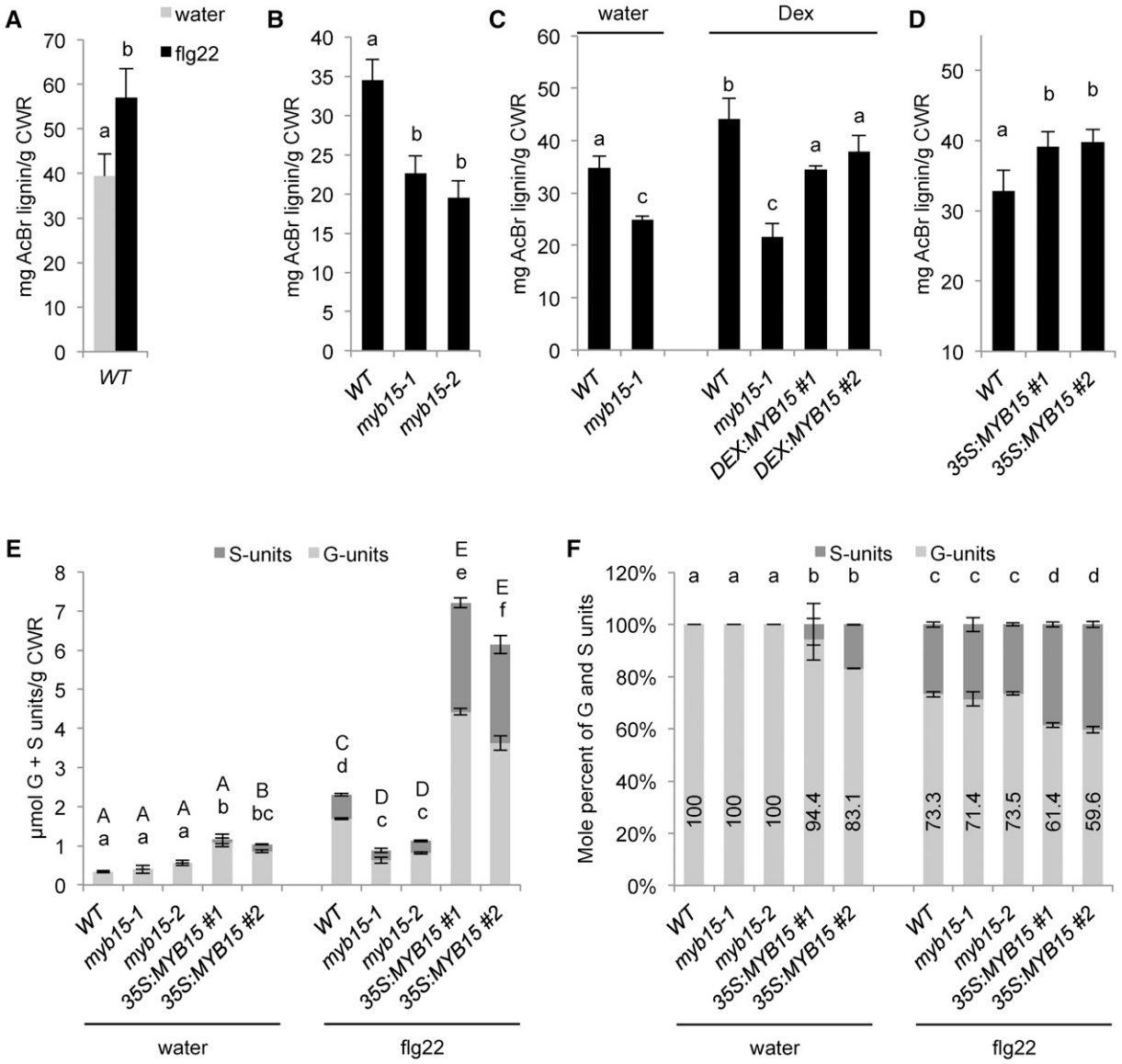

Figure 2. *MYB15* Is Sufficient to Activate flg22-Induced Lignification.

(A) to **(D)** Lignin analysis by AcBr method. Data represent the mean ± SD of six (**[A]** and **[B]**), three **(C)**, and eight **(D)** replicates of 30 to 45 seedlings each. Different letters denote statistically significant differences ($P < 0.05$, two-tailed *t* test). Experiments were repeated once or twice, producing similar results.

(A) Nine-day-old seedlings elicited with water or 2 μM flg22 for 48 h.

(B) and **(D)** Unelicited 10-d-old seedlings.

(C) Nine-day-old seedlings treated with water or 20 μM Dex for 48 h.

(E) and **(F)** Lignin analysis by DFRC method. Nine-day-old seedlings elicited with water or 2 μM flg22 for 48 h. Data represent the mean ± SD of three replicates of 30 to 45 seedlings each. Different letters denote statistically significant differences ($P < 0.05$, two-tailed *t* test).

(Meyer et al., 1998), which is involved in the branch of the monolignol pathway that generates the S-units. Upregulation of F5H activity diverts flux away from G-lignin biosynthesis toward S-lignin (Supplemental Figure 1), resulting in lignin with higher S/G molar ratios. To determine whether MYB15 activates *F5H* expression, we measured *F5H* transcript levels in the wild type, *myb15* mutants, and *MYB15*-overexpressing lines by qPCR. Consistent with our lignin analysis, all 11 genes in the monolignol pathway, including *F5H*, are upregulated in wild-type seedlings in response to 1 μM flg22 for 3 h (Figures 3A and 3B). *F5H* transcript levels are also similarly regulated in flg22-elicited *myb15-1* and *myb15-2* mutants (Figures 3B and 3C) and in unelicited *MYB15*-overexpressing lines (Figures 3B and 3D). By contrast, the expression of all other monolignol pathway genes are significantly reduced in flg22-elicited *myb15* mutants (Figures 3B and 3C) and increased in unelicited *MYB15*-overexpresssing lines compared

with the wild type (Figures 3B and 3D). Interestingly, MYB58 also activates all monolignol pathway genes except *F5H* in the developing stem (Zhou et al., 2009), lending further support that SG2-type and SG3-type R2R3-MYBs are functionally related. Together with our lignin analysis, these findings indicate that MYB15 mediates defense-induced synthesis of G-lignin, but not S-lignin.

In the developing stem, *F5H* is activated by MYB103 transcription factor (Öhman et al., 2013). However, *MYB103* and its close homologs *MYB67* and *MYB26* (Supplemental Figure 4) are not upregulated in wild-type seedlings in response to flg22 treatment (Denoux et al., 2008; data not shown). Thus, the gene pathway regulating defense-induced synthesis of S-lignin remains unknown.

MYB15 Binds to Gene Promoters Required for G-Lignin Biosynthesis

MYB15 reportedly binds to type IIG [(T/C)ACC(A/T)A(A/C)C] Myb recognition sequences in electrophoretic mobility shift assays (Romero et al., 1998; Agarwal et al., 2006). This recognition sequence encompasses the 7-bp secondary wall MYB-responsive element (SMRE) [ACC(A/T)A(A/C)(T/C)] that is recognized by SG13-type R2R3-MYBs to drive secondary cell wall biosynthesis (Zhong and Ye, 2012). This SMRE consensus sequence in turn encompasses the three AC elements, AC-I (ACCTACC), AC-II (ACCAACC), and AC-III (ACCTAAC), that are present in nearly all monolignol pathway gene promoters except the *COMT* gene promoter (Supplemental Table 1) (Raes et al., 2003). In addition to the AC elements, three SMREs, SMRE-1 (ACCAAAT), SMRE-2 (ACCAACT), and SMRE-3 (ACCAAAC), are present in the majority of monolignol pathway gene promoters including the *COMT* gene promoter, which contains a single SMRE-1.

To determine whether MYB15 directly binds to AC/SMRE-containing regions of monolignol pathway gene promoters, we performed chromatin immunoprecipitation (ChIP) on 4-h mock- and Dex-treated *myb15-1/DEX:MYB15-myc* seedlings using antibodies specific to myc (Supplemental Figure 6). After immunoprecipitation, PCR was used to amplify AC/SMRE-containing regions within 1000 bp upstream of the translational start site of all 11 genes in the monolignol pathway and the scopoletin biosynthetic gene *F6'H1*. MYB15 binds strongly (>10-fold enrichment) to the AC-II/III and SMRE-2/3-containing regions (Supplemental Table 1) of the *PAL1* and *C4H* gene promoters (Figure 4) and the SMRE-1-containing region of the *COMT* gene promoter (Figure 4). By comparison, MYB15 binds weakly (1.5- to 10-fold enrichment) to the AC-I/II and SMRE-1/2-containing regions (Supplemental Table 1) of the *HCT*, *CCoAOMT1*, *CSE*, and *CAD5* gene promoters (Figure 4). MYB15 did not bind to the AC-I/II/III and SMRE-3-containing regions of the *4CL1*, *C3H*, *CCR1*, and *F5H* promoters (Figure 4), nor did it bind to the SMRE-1-containing region of the *F6'H1* promoter (Figure 4). These results are consistent with the proposed role of AC elements as the common *cis*-regulatory elements driving the coordinated expression of G-lignin biosynthesis in vascular cells (Hatton et al., 1995; Raes et al., 2003) and suggest that SMREs may also contribute to the transcriptional regulation of lignin biosynthesis.

MYB15-Dependent Synthesis of G-Lignin Contributes to Basal Immunity

To evaluate whether *MYB15* and other specific regulators of lignin biosynthesis contribute to Arabidopsis basal immunity, we challenged *myb15*, *myb58*, and *myb63* mutants with the virulent bacterial pathogen *P. syringae* pv *tomato* DC3000 (*Pto* DC3000). Whole seedlings and adult leaves of *myb15* mutants, but not *myb58* and *myb63*, are both more susceptible to *Pto* DC3000 infection (Figure 5A). Their immune-deficient phenotypes are comparable to the *fls2* mutant lacking the functional flg22 receptor (Figure 5A). Consistent with *MYB15*'s role in basal disease resistance against a bacterial pathogen, Dex-induced expression of *MYB15* restores basal resistance in *myb15-1* seedlings and adult leaves to wild-type levels (Figure 5B).

To determine whether defense-induced lignification contributes to basal immunity, we performed lignin analysis and bacterial infection assays on lignin biosynthetic mutants. In the stem, the loss of PAL1, CSE, or CCR1 all result in reductions in overall lignin content (Jones et al., 2001; Rohde et al., 2004; Vanholme et al., 2013) but with differential effects on the S/G molar ratio. Namely, the S/G molar ratio is wild-type in the *pal1-3* mutant (Rohde et al., 2004), increased in the *cse-2* mutant (mainly due to a reduction in G-units; Vanholme et al., 2013), and decreased in the *ccr1-6* mutant (mainly due to a decrease in S-units; Van Acker et al., 2013). By contrast, the *fah1-2* mutant, deficient in F5H activity and S-lignin, accumulates wild-type levels of total lignin, with all flux to S-lignin redirected to G-lignin (Meyer et al., 1998). Consistent with the reported G-lignin content, the *pal1-3* and *cse-2*, but not the *ccr1-6* and *fah1-2*, display reduced flg22-induced lignin responses by phloroglucinol-HCl staining (Figure 5C). In addition, seedlings and adult leaves of *pal1-3*, *cse-2*, and *ccr1-6* mutants are more susceptible to *Pto* DC3000 infection than wild-type plants (Figure 5D). Since CCR1 catalyzes the first specific step in the synthesis of monolignols (Supplemental Figure 1), this finding supports a general role for defense-induced lignification in basal immunity.

Our lignin composition analysis indicated that defense-induced synthesis of S-lignin occurs independently of MYB15 (Figure 2E). To determine which major component of defense-induced lignin, G or S, contributes to basal immunity against a hemibiotroph, we performed bacterial infection assays on S-lignin mutants *fah1-2* (*f5 h*) and *omt1-2* (*comt*) and found they have a wild-type level of resistance to *Pto* DC3000 (Figure 5D), providing genetic evidence that S-lignin does not contribute to basal immunity. Together, our results support a specific role of MYB15-dependent G-lignin biosynthesis in basal immunity.

MYB15 Activates Synthesis of Soluble Phenolics Independently of Immune Activation

The monolignol pathway also underpins the synthesis of a number of defense-inducible soluble phenolics such as the hydroxycinnamic acid esters (HCAEs), hydroxycinnamic acid amides (HCAAs), and coumarins (Supplemental Figure 1). AACT1, F6'H1, and UGT84A1-4 catalyze the first specific steps in branch pathways synthesizing HCAAs, the coumarin scopoletin and HCAEs, respectively (Lim et al., 2001; Kai et al., 2008; Muroi et al., 2009;

A

Locus	Gene	Fold Change	*P* value
At2g37040	*PAL1*	30.4	$5x10^{-10}$
At2g30490	*C4H*	16.5	$5.4x10^{-6}$
At1g51680	*4CL1*	13.6	$9x10^{-6}$
At5g48930	*HCT*	2.7	$3.6x10^{-6}$
At2g40890	*C3'H*	3.4	$1.8x10^{-9}$
At1g52760	*CSE*	6.5	$2.1x10^{-6}$
At4g34050	*CCoAOMT1*	2.9	$1.7x10^{-4}$
At1g15950	*CCR1*	2.5	$6.1x10^{-5}$
At4g34230	*CAD5*	11.8	$5.1x10^{-8}$
At4g36220	*F5H/FAH1*	4.8	$2.1x10^{-6}$
At5g54160	*COMT*	4.9	$1.7x10^{-4}$
At5g61160	*AACT1*	6.4	$3.5x10^{-6}$
At3g13610	*F6'H1*	4.1	$3.2x10^{-7}$
At4g15480	*UGT84A1*	4.5	$8.7x10^{-3}$

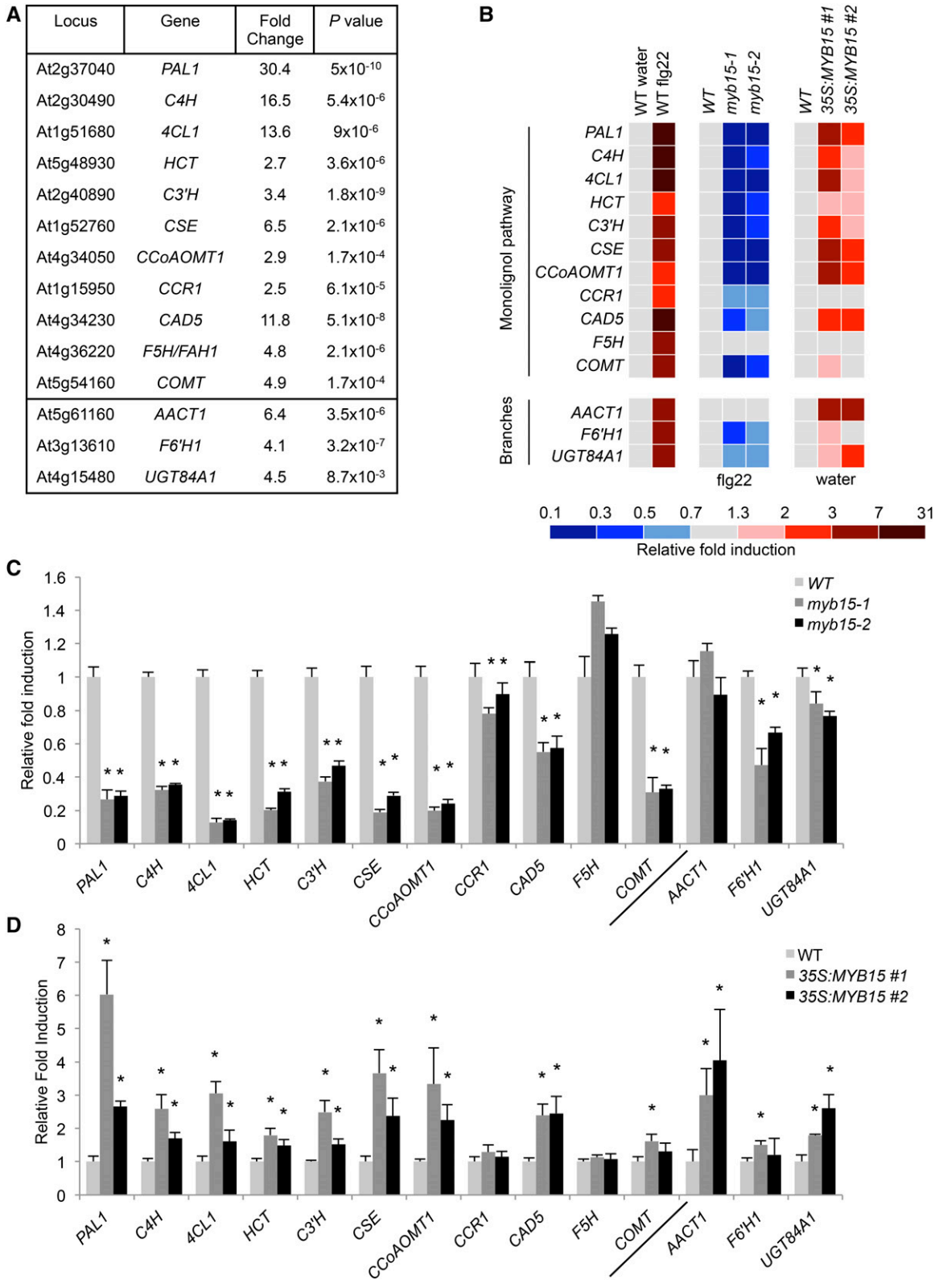

Figure 3. MYB15 Activates Genes Involved in the Biosynthesis of G-Lignin, Not S-Lignin.

(A) Table of monolignol and branch pathway genes transcriptionally activated in response to flg22 elicitation. Nine-day-old wild-type seedlings elicited with water or 1 μM flg22 for 3 h. Expression values are normalized to that of *eIF4A1* housekeeping gene and relative to those of water-treated wild-type sample. Data represent mean of four replicates of 10 to 15 seedlings each. P value determined by two-tailed *t* test.

(B) Heat map of relative gene expression levels of monolignol and branch pathway genes in **(C)** and **(D)**.

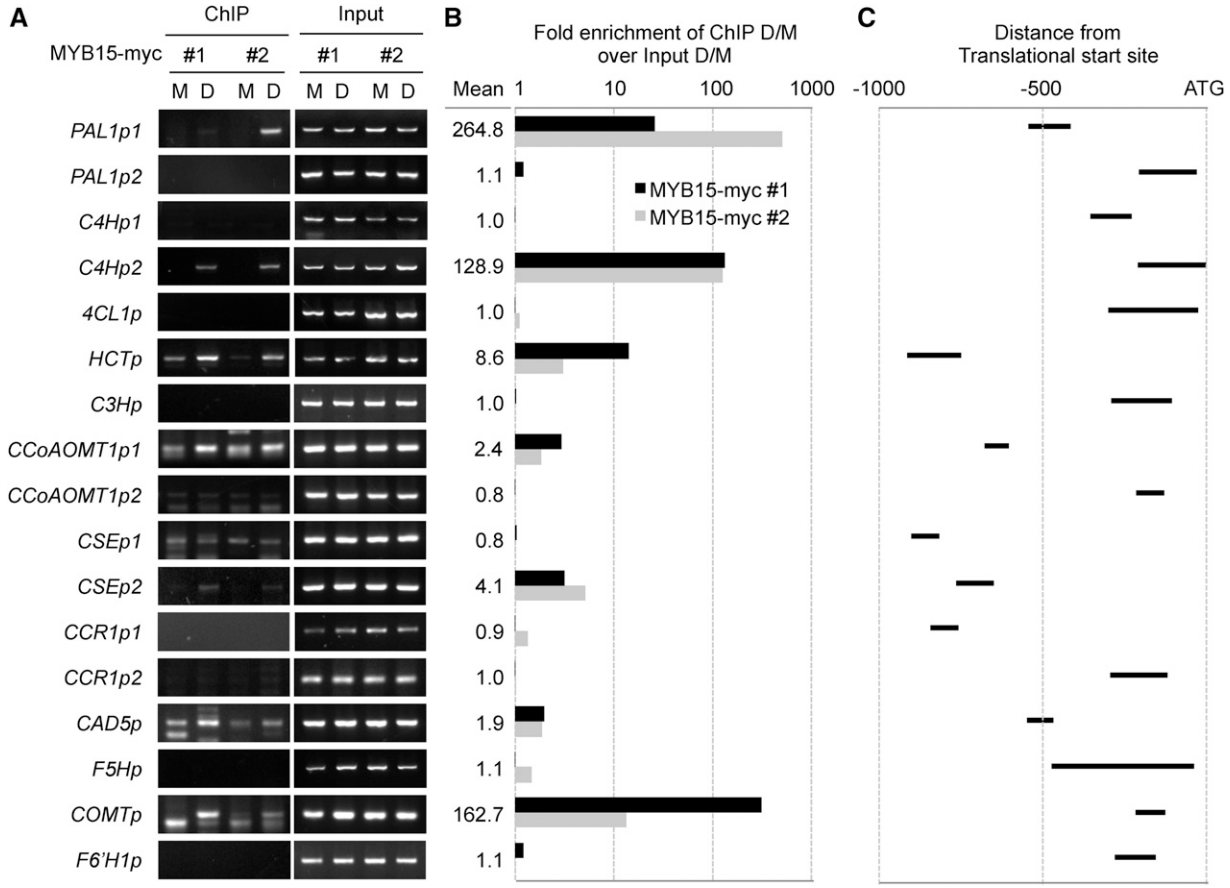

Figure 4. MYB15 Binds to Promoters of Monolignol Pathway Genes.

(A) ChIP was performed on 8-d-old *myb15-1* seedlings containing *DEX:MYB15-myc* transgene and pretreated with mock solution (M) or 20 μM Dex (D) for 4 h. PCR analysis was performed on nuclear extracts prior to incubation with myc antibody (input) and after ChIP, using primers flanking regions containing AC-like *cis*-elements (listed in Supplemental Table 2).

(B) Fold enrichment was determined by calculating the ratio of PCR product intensities in ChIP D/M to Input D/M. The mean fold enrichment of two independent immunoprecipitation experiments is reported to the left of the graph.

(C) Schematic representations of monolignol pathway gene promoters with the amplified regions represented by black bars. Numbers indicate nucleotide positions upstream of the translational start site.

Supplemental Figure 1). To investigate whether their synthesis is also regulated by MYB15, we measured *AACT1*, *F6'H1*, and *UGT84A1* transcript levels in wild-type, *myb15* mutant, and *MYB15*-overexpressing plants by qPCR. Consistent with previous transcriptomic study (Denoux et al., 2008), all three genes are upregulated in wild-type seedlings in response to 1 μM flg22 for 3 h (Figures 3A and 3B). Loss of MYB15 function decreases flg22-induced expression of *UGT84A1* and *F6'H1* (Figures 3B and 3C), whereas overexpression of *MYB15* increases unelicited expression of *AACT1*, *UGT84A1*, and *F6'H1* (Figures 3B and 3D). These results suggest that MYB15 also transcriptionally activates the production of HCAEs, HCAAs, and coumarins.

Figure 3. (continued).

(C) qPCR analysis of monolignol and branch pathway genes in 9-d-old seedlings elicited with 1 μM flg22 for 3 h. Expression values are normalized to that of *eIF4A1* housekeeping gene and relative to those of flg22-treated wild-type sample. Data represent mean ± SD of four replicates of 10 to 15 seedlings each. Asterisks denote statistically significant differences from the wild type ($P < 0.05$, two-tailed *t* test; false discovery rate < 0.05).

(D) qPCR analysis of monolignol and branch pathway genes in unelicited 9-d-old seedlings. Expression values are normalized to that of *eIF4A1* housekeeping gene and relative to those of wild-type sample. Data represent mean ± SD of four replicates of 10 to 15 seedlings each. Asterisks denote statistically significant differences from the wild type ($P < 0.05$, two-tailed *t* test; false discovery rate < 0.05). qPCR experiments were repeated once, producing similar results.

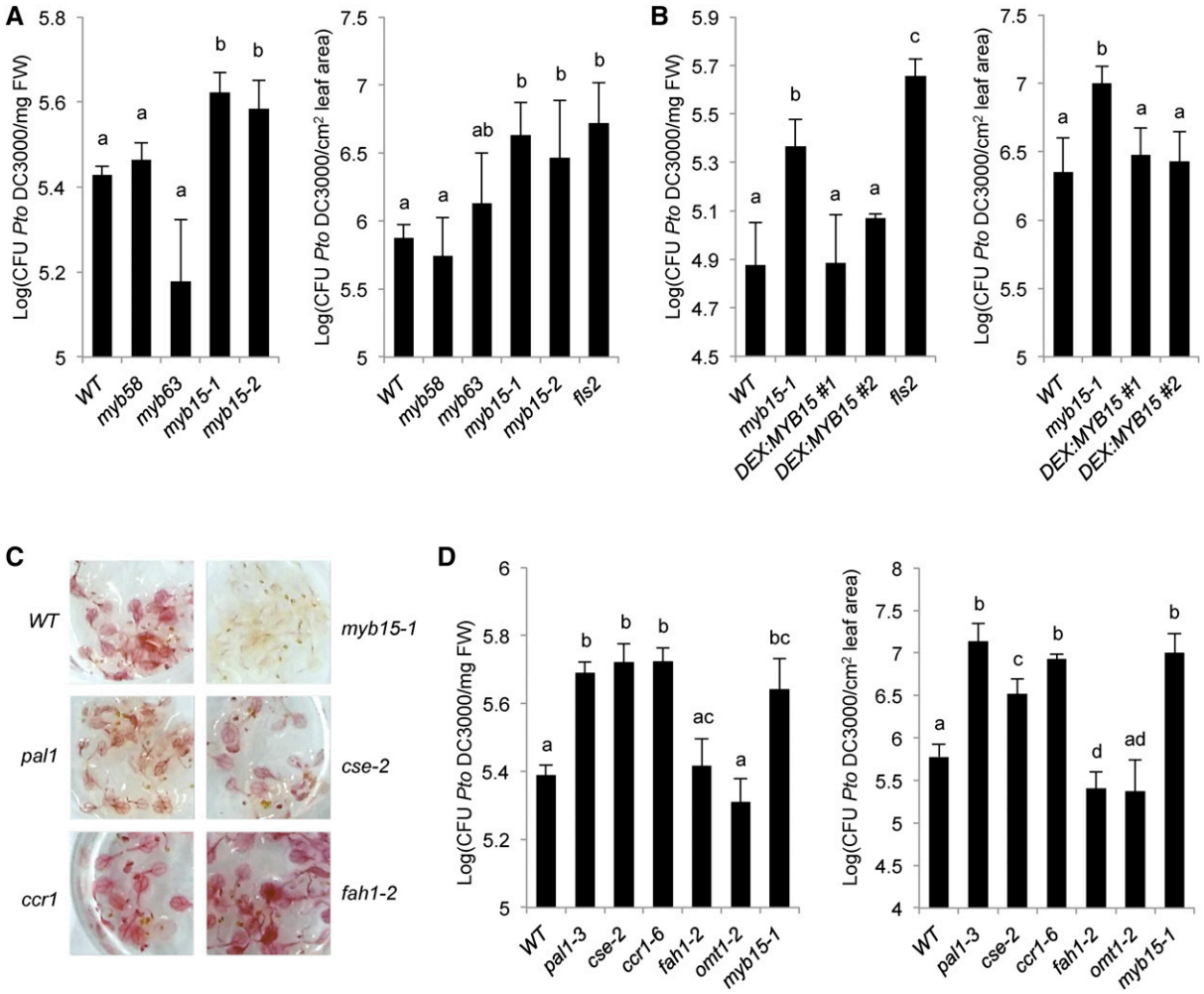

Figure 5. MYB15-Dependent Synthesis of G-Lignin Contributes to Basal Resistance against the Virulent Bacterial Pathogen *P. syringae*.

(A), **(B)**, and **(D)** Pathogen infection assays in 10-d-old seedlings (left) and 5-week-old leaves (right). Bacteria were extracted from untreated plants (**[A]** and **[C]**) and from plants treated with 20 μM Dex for 6 h prior to surface-inoculation with *Pto* DC3000 **(B)**. Data represent the mean ± SD of five (**[A]**, left; **[B]**, left; **[D]**, left), four (**[D]**, right), and three (**[A]**, right; **[B]**, right) replicates. Different letters denote statistically significant differences ($P < 0.05$, two-tailed *t* test). FW, fresh weight. Experiments were repeated once or twice, producing similar results.

(C) Lignin analysis by phloroglucinol-HCl staining of 9-d-old seedlings elicited with 1 μM flg22 for 48 h.

To confirm MYB15's role in the production of defense-inducible soluble phenolics, we measured their abundance in wild-type, *myb15* mutant, and *MYB15*-overexpressing plants by untargeted liquid chromatography-tandem mass spectrometry (LC-MS/MS). The major defense-inducible HCAAs in Arabidopsis are *p*-coumaroylagmatine (**C1**), feruloylagmatine (**C2**), *p*-coumaroylputrescine (**C3**), and feruloylputrescine (**C4**) (Supplemental Figure 1); their combined accumulation is correlated with increased resistance to the necrotrophic fungus *Alternaria brassicicola* (Muroi et al., 2009). Consistent with flg22-activated expression of *AACT1* in wild-type and *myb15* mutants (Figures 3A and 3B), the levels of HCAAs coumaroylagmatine, feruloylagmatine, and coumaroylputrescine are increased in wild-type seedlings in response to 1 μM flg22 for 24 h (Figure 6B; Supplemental Figure 7) and unchanged or increased in *myb15* mutants (Figure 6B; Supplemental Figure 7). These findings indicate that defense-induced HCAA biosynthesis is independent of *MYB15*.

The major coumarins in Arabidopsis are scopoletin (**D1**) and its glucoside (**D2**) (Supplemental Figure 1) (Kai et al., 2006). Contrary to previous metabolomics study on flg22-elicited cell cultures (Schenke et al., 2011) and flg22-activated expression of *F6'H1* (Figures 3A and 3B), the levels of scopoletin and its glucoside conjugate (**D2**; Supplemental Figure 1) are unchanged in flg22-elicited wild-type seedlings (Figure 6B; Supplemental Figure 7). However, scopoletin levels are reduced in flg22-elicited *myb15* mutants compared with elicited wild-type and unelicited *myb15* plants (Figure 6B; Supplemental Figure 7). Conversely, *MYB15* overexpression increases the synthesis and accumulation of scopoletin and its glucoside independently of immune activation

A

Identifier	Compound	Mass	RT (min)	*m/z*
A1	phenylalanine	165.079	1.84	166.084
B1	*p*-coumaric acid	164.047	7	165.055
B2	1-sinapoylglucose isomer 1	386.1184	8.02	387.1261
B3	1-sinapoylglucose isomer 2	386.1185	8.72	387.1261
B4	1,2-disinapoylglucose	592.1738	15.20	593.181
C1	coumaroylagmatine	276.1568	8.31	277.1642
C2	feruloylagmatine	306.1692	9.25	307.1764
C3	coumaroylputrescine	234.1368	5.68	235.144
C4	feruloylputrescine	264.1474	6.45	265.1546
D1	scopoletin	192.0413	10.68	193.0486
D2	scopoletin glucoside	354.0925	7.17	355.1001

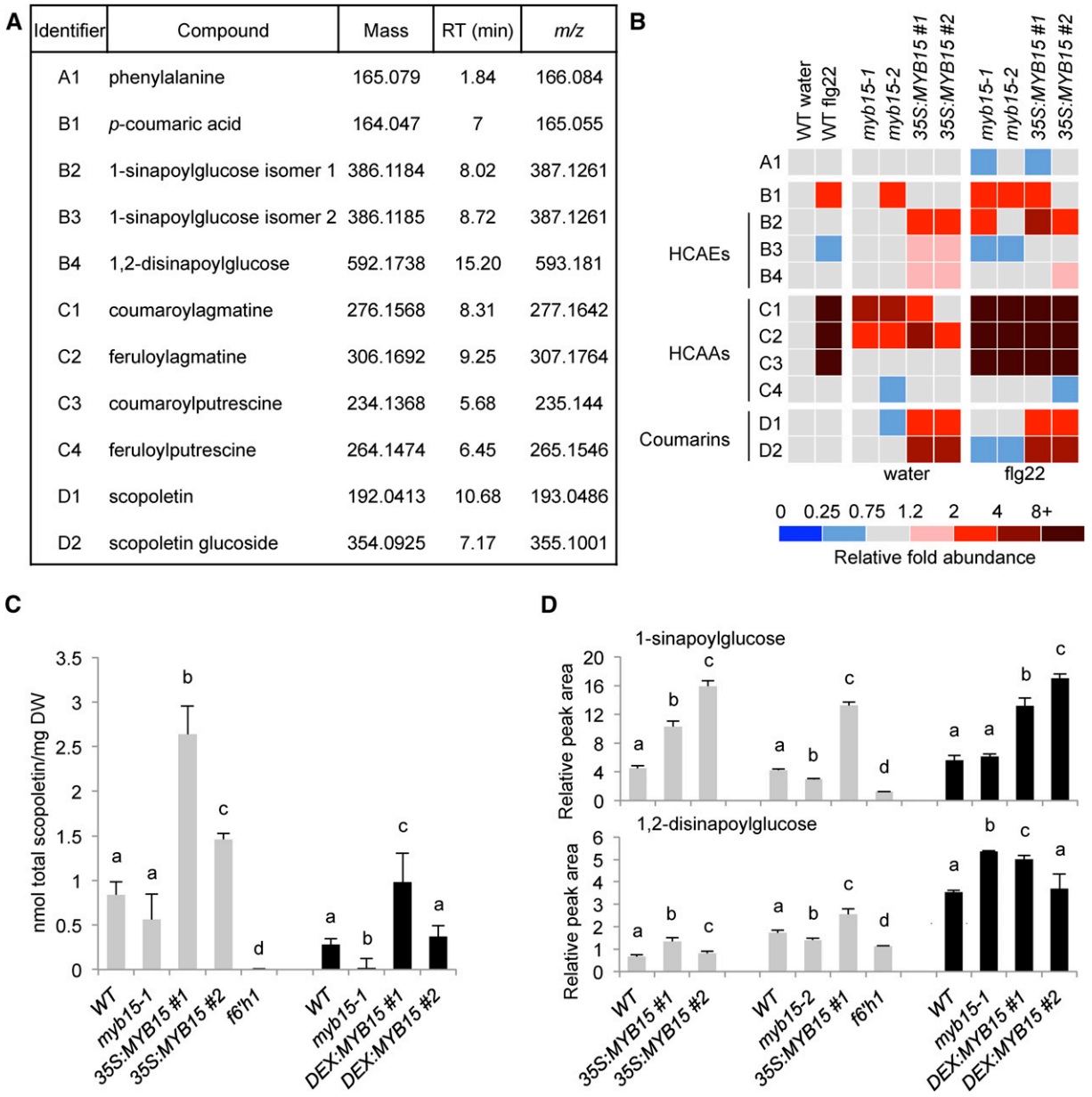

Figure 6. MYB15 Increases the Synthesis of Soluble Phenolics Independently of flg22.

(A) Table of soluble phenolics detected in 10-d-old wild-type seedlings by LC-MS/MS and whose identities were inferred from accurate *m/z* measurements of high-resolution mass spectrometry data and confirmed by their absence in biosynthetic mutants *f6'h1*, *fah1-2*, and *aact1-1*. RT, retention time.

(B) Heat map of relative abundances of soluble phenolics in 10-d-old seedlings elicited with water or 1 μM flg22 for 3 h. Data representing mean ± SD of five replicates can be found in Supplemental Figure 7.

(C) HPLC-FLD analysis of total scopoletin in 9-d-old seedlings, either unelicited (left) or treated with 20 μM Dex for 24 h (right). Data represents the mean ± SD of four replicates of 10 to 15 seedlings each. Different letters denote statistically significant differences ($P < 0.05$, two-tailed *t* test).

(D) HPLC-DAD analysis of sinapate esters in 9-d-old seedlings, either unelicited (left and center) or treated with 20 μM Dex for 24 h (right). Peak area values are normalized to that of internal standard. Data represents the mean ± SD of four replicates of 10 to 15 seedlings each. Different letters denote statistically significant differences ($P < 0.05$, two-tailed *t* test). HPLC experiments were repeated at least once, producing similar results.

(Figure 6B; Supplemental Figure 7). To confirm scopoletin biosynthesis is MYB15-dependent, we measured total scopoletin (free and conjugated) levels in *myb15* mutants, *MYB15*-overexpressing lines, and inducible *MYB15*-expressing lines by HPLC-DAD. Scopoletin amounts can vary in response to environmental stresses (Kai et al., 2006). At basal levels, the *myb15* mutant accumulates significantly less total scopoletin than the wild type (Figure 6C), consistent with our LC-MS/MS data on unelicited *myb15* plants (Figure 6B; Supplemental Figure 7). In addition, *MYB15* overexpression and Dex-induced *MYB15* expression increase accumulation of total scopoletin in wild-type plants and *myb15-1* plants, respectively (Figure 6C). These findings indicate that *MYB15* contributes to scopoletin biosynthesis independently of immune activation.

The major defense-inducible HCAEs (or sinapate esters) in Arabidopsis are 1-sinapoylglucose (**B2/B3**) and 1,2-disinapoylglucose (**B4**) (Supplemental Figure 1) (König et al., 2014). The accumulation of 1-sinapoylglucose is correlated with increased resistance to the hemibiotrophic fungus *Verticillium longisporum* (König et al., 2014). Contrary to flg22-activated expression of *UGT84A1* (Figures 3A and 3B), flg22 elicitation reduces or has no effect on the levels of 1-sinapoylglucose and 1,2-disinapoylglucose, respectively, in wild-type and *myb15* seedlings (Figure 6B; Supplemental Figure 7). Even though sinapate ester levels are unchanged in elicited wild-type and *myb15* plants, *MYB15*-overexpressing lines overaccumulate 1-sinapoylglucose and 1,2-disinapoylglucose independently of immune activation (Figure 6B; Supplemental Figure 7). To confirm that sinapate ester biosynthesis is not MYB15-dependent, we measured the levels of 1-sinapoylglucose and 1,2-disinapoylglucose in *myb15* mutants, *MYB15*-overexpressing lines, and inducible *MYB15*-expressing lines by HPLC-DAD. The *myb15* mutants accumulate slightly less to wild-type levels of 1-sinapoylglucose (Figure 6D) and highly variable levels of 1,2-disinapoylglucose (Figure 6D). The variability in sinapate ester levels in *myb15* mutants rules out *MYB15* playing a significant role in the biosynthesis of defense-inducible sinapate esters. These results are largely consistent with the LC-MS/MS data on the *myb15* mutants (Figure 6B; Supplemental Figure 7). Also consistent with the LC-MS/MS data, *MYB15* overexpression increases the accumulation of 1-sinapoylglucose and 1,2-disinapoylglucose in wild-type plants (Figure 6D), while Dex-induced *MYB15* expression increases the accumulation of only 1-sinapoylglucose in *myb15-1* mutant plants (Figure 6D). These findings suggest that *MYB15* does not contribute significantly to sinapate ester biosynthesis, although it can activate their biosynthesis, possibly by increasing flux to the monolignol pathway.

Scopoletin Contributes to Plant Defense Independently of Immune Activation

To evaluate whether defense-inducible HCAAs and MYB15-dependent scopoletin contribute to Arabidopsis defense, we performed bacterial infection assays on the *aact1-1* and *f6'h1-1* mutants, which are deficient in HCAAs and scopoletin, respectively (Kai et al., 2008; Muroi et al., 2009). Seedlings and adult leaves of the *aact1-1* mutant have a wild-type level of resistance to *Pto* DC3000 (Figures 7A and 7B), indicating that HCAAs do not play a role in antibacterial defense. By contrast, seedlings and adult leaves of the *f6'h1* mutant are more susceptible to *Pto* DC3000 infection compared with the wild type (Figures 7A and 7B). Its immune-deficient phenotype is comparable to that of the *myb15-1* mutant (Figures 7A and 7B). This finding suggests that scopoletin contributes to antibacterial defense (Figure 7C).

Unlike G-lignin, the soluble phenolic scopoletin can be used to test for a direct role in the plant innate immune response, either as defense-inducible antibacterial or signaling compound, by pre-immunizing wild-type adult leaves a physiological amount of scopoletin prior to infection with *Pto* DC3000 and measuring scopoletin's protective effect in the presence or absence of flg22 elicitation. Unelicited 4-week-old Arabidopsis leaves are reported to accumulate 0.072 nmol scopoletin and 6.87 nmol scopoletin glucoside per gram fresh weight, or 0.002 nmol scopoletin and 0.21 nmol scopoletin glucoside per leaf (assuming the average 4-week-old leaf weighs 30 mg). By contrast, leaves infected with the fungal pathogen *Fusarium oxysporum* accumulate 0.68 nmol scopoletin and 16 nmol scopoletin glucoside per gram fresh weight, or 0.02 nmol scopoletin and 0.48 nmol scopoletin glucoside per leaf (Kai et al., 2006). Infiltration of unelicited leaves with 0.05 nmol of scopoletin per leaf does not alter the wild-type level of resistance compared with the solvent control (Figure 7C, left). However, cotreatment of leaves with scopoletin and flg22 confers greater susceptibility to bacterial infection than the solvent control, biosynthetically related phenolic ferulic acid, and non-native coumarin umbelliferone (Figure 7C). Since scopoletin and its glucoside do not accumulate in the plant in response to flg22 elicitation (Figure 6B; Supplemental Figure 7), our findings altogether suggest that scopoletin contributes to antibacterial defense independently of immune activation (Figure 7D) and may even adversely affect basal immunity.

MYB13 and *MYB14* Do Not Regulate Defense-Induced Lignification

In addition to MYB15, Arabidopsis contains two additional SG2-type R2R3-MYBs, MYB14 and MYB13 (Stracke et al., 2001) (Supplemental Figures 3 and 4). Of the three transcription factors, only *MYB15* is upregulated more than 2-fold in wild-type seedlings in response to 1 μM flg22 for 3 h (Figure 8A). In addition, *MYB13* and *MYB14* gene expression is unaffected in *myb15* mutants in the presence or absence of flg22 elicitation (Figure 8B), suggesting that MYB15 functions independently of MYB13 and MYB14. Like *myb15*, the *myb13* and *myb14* T-DNA insertion mutants (Supplemental Figure 8), have normal vegetative growths (Supplemental Figure 5C) and slightly reduced inflorescence stem growths (Supplemental Figures 5B and 5D). To determine the extent of functional redundancy among the SG2-type R2R3-MYBs, we generated double and triple mutants by intermutant crosses of the single mutants. The *myb13* and *myb14* single mutants; the *myb13 myb14* (*myb13/14*), *myb14 myb15* (*myb14/15*), and *myb13 myb15* (*myb13/15*) double mutants; and the *myb13 myb14 myb15* (*myb13/14/15*) triple mutant have normal vegetative growth and slightly reduced inflorescence growth (Supplemental Figures 5C and 5D), resembling the *myb15* single mutant. In addition, the *myb13* and *myb14* single mutants and the *myb13/14* double mutant exhibit a wild-type level of flg22-induced lignin response (Figure 8C) and *PAL1* gene expression (Figure 8D), indicating that defense-induced lignification is not affected in these mutants. The *myb13/15* and *myb14/15* double mutants and the *myb13/14/15* triple mutant resemble the single *myb15* mutant both in the flg22-induced lignin

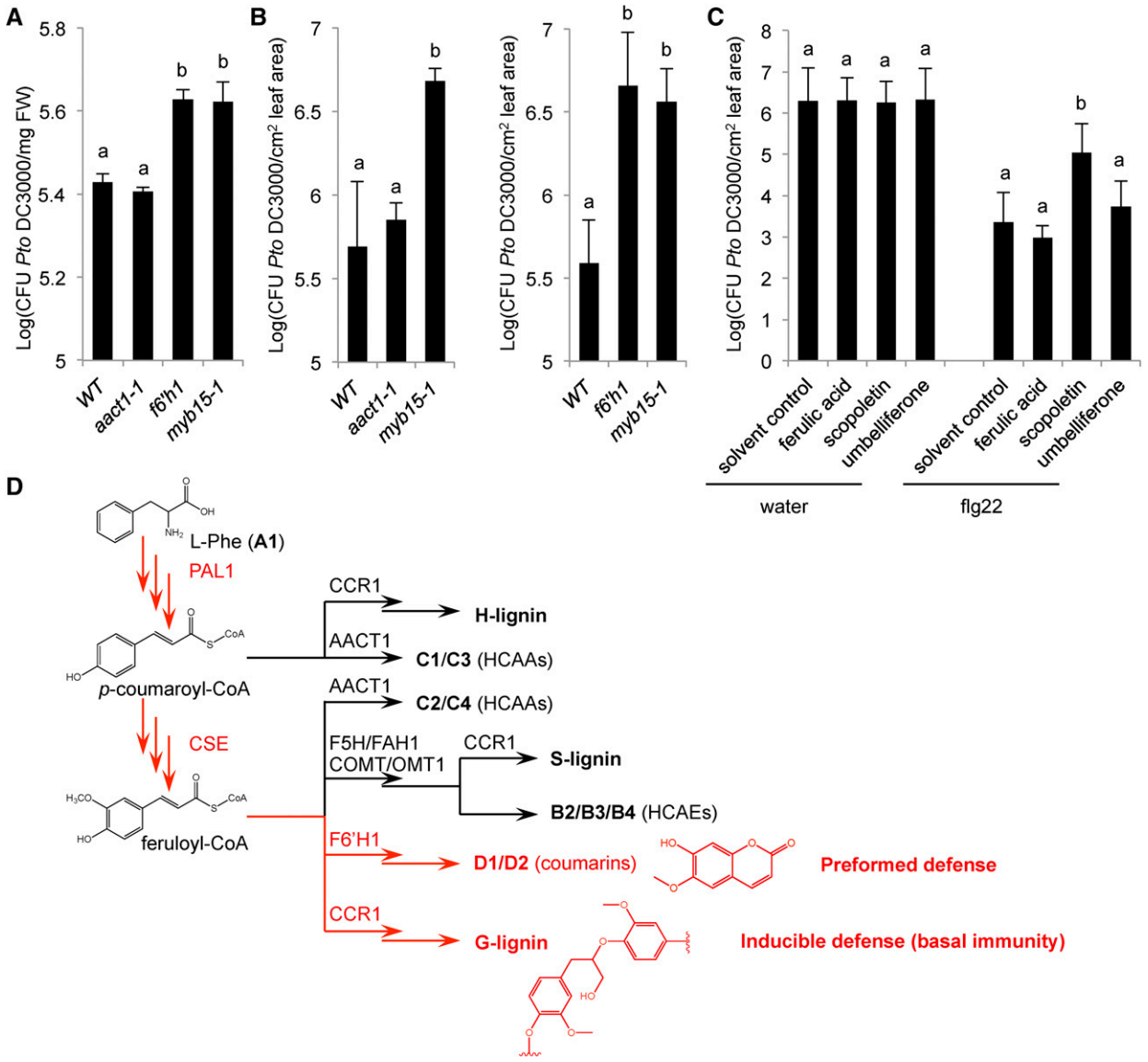

Figure 7. Scopoletin Contributes to Antibacterial Defense Independently of Immune Activation.

(A) to **(C)** Pathogen infection assays in 10-d-old seedlings **(A)** and 5-week-old leaves (**[B]** and **[C]**). Bacteria were extracted from plants surface-inoculated with *Pto* DC3000 (**[A]** and **[B]**) and from leaves preinfiltrated with 0.1 nmol flg22 and 0.05 nmol soluble phenolic per leaf for 24 h prior to infiltration with *Pto* DC3000 **(C)**. Data represent the mean ± SD of three **(A)**, four **(B)**, six (**[C]**, left), and eight (**[C]**, right) replicates. Different letters denote statistically significant differences ($P < 0.05$, two-tailed *t* test). FW, fresh weight. Experiments were repeated once (**[A]** and **[B]**) or twice **(C)**, producing similar results.
(D) Schematic of monolignol and branch pathways involved in preformed and inducible defenses against a bacterial pathogen (red).

response (data not shown) and *PAL1* gene expression (Figure 8D). Together, the results suggest that *MYB13* and *MYB14* do not contribute significantly to defense-induced lignification.

DISCUSSION

SG2-Type R2R3-MYBs in Phenylpropanoid Metabolism and Basal Immunity

SG2-type R2R3-MYBs were first characterized by their activation of *PAL* expression in response to various biotic stresses, including wounding and microbial elicitors (Sugimoto et al., 2000; Maeda et al., 2005). Later studies identified SG2 R2R3-MYBs as regulators of the production of clade-specific, defense-inducible soluble phenolics from the isoflavonoid and stilbenoid pathways in lotus (*Lotus japonicus*) and grapevine (*Vitis vinifera*), respectively, in response to abiotic stress (Shelton et al., 2012; Höll et al., 2013), as well as regulators of cold stress-induced lignification in loquat (Xu et al., 2014). We show MYB15 as necessary for defense-induced lignification. Consistent with our findings, MYB15 reportedly activates the shikimate pathway (Chen et al., 2006), which functions upstream of phenylpropanoid metabolism. MYB15 also mediates harpin $HrpN_{EA}$-induced resistance

A

Locus	Gene	Fold Change	P-value
At3g23250	*MYB15*	13.9	$1.4x10^{-6}$
At1g06180	*MYB13*	1.63	0.006
At2g31180	*MYB14*	1.49	0.009

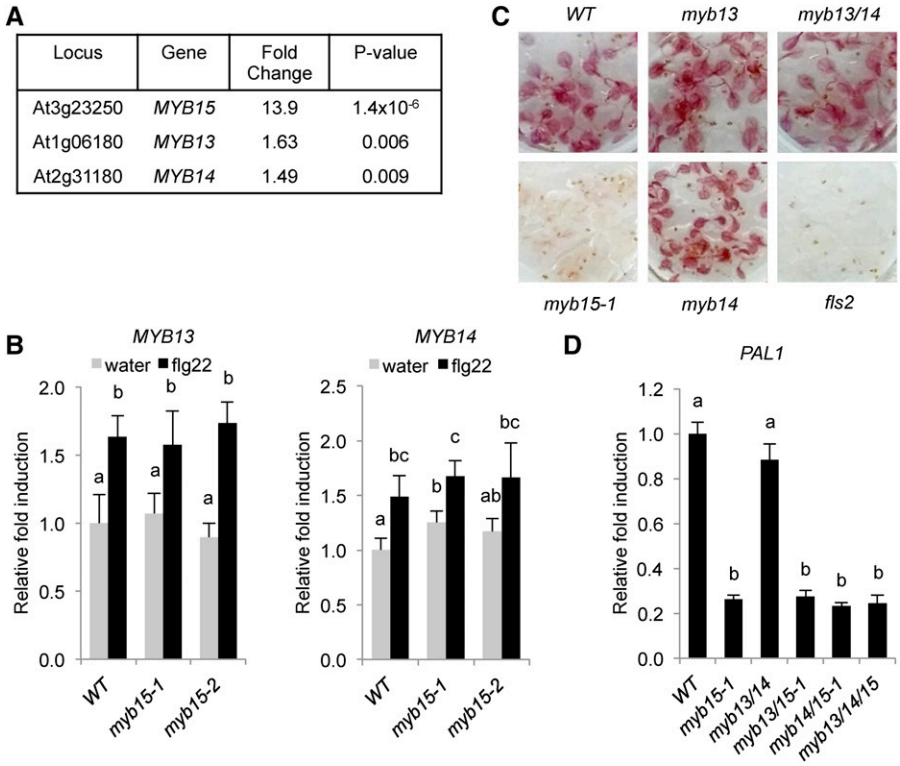

Figure 8. *MYB15* Paralogs *MYB13* and *MYB14* Do Not Contribute to Defense-Induced Lignification.

(A) Table of SG2-type R2R3-MYB genes transcriptionally activated in response to flg22 elicitation. Nine-day-old wild-type seedlings elicited with water or 1 μM flg22 for 3 h. Expression values are normalized to that of *eIF4A1* housekeeping gene and relative to those of water-treated wild-type sample. Data represent mean of four replicates of 10 to 15 seedlings each. P value determined by two-tailed *t* test.

(B) qPCR analysis of *MYB13* and *MYB14* genes in 9-d-old seedlings elicited with water or 1 μM flg22 for 3 h. Expression values are normalized to that of *eIF4A1* housekeeping gene and relative to those of water-treated wild-type sample. Data represent mean ± SD of four replicates of 10 to 15 seedlings each. Different letters denote statistically significant differences ($P < 0.05$, two-tailed *t* test).

(C) Lignin analysis by phloroglucinol-HCl staining. Nine-day-old seedlings elicited with 1 μM flg22 for 48 h.

(E) qPCR analysis of *PAL1* gene in 9-d-old seedlings elicited with 1 μM flg22 for 3 h. Expression values are normalized to that of *eIF4A1* housekeeping gene and relative to those of wild-type sample. Data represent mean ± SD of four replicates of 10 to 15 seedlings each. Different letters denote statistically significant differences ($P < 0.05$, two-tailed *t* test).

to the phloem-feeding green peach aphid (Liu et al., 2010; Dong et al., 2004), possibly by linking ethylene signaling (Dong et al., 2004; Yanhui et al., 2006) to phenylpropanoid metabolism. Because $HrpN^{EA}$ is secreted by the bacterial necrotrophic pathogen *Erwinia amylovora*, necrotrophs may promote disease development by using MYB15 among others to divert plant defense responses such as phenylpropanoid metabolism toward (hemi)biotrophs. These studies support a universal role of SG2-type R2R3-MYBs in stress-induced phenylpropanoid metabolism in seed plants.

The role of SG2-type R2R3-MYBs in preformed plant defense is less known. MYB15 is also necessary for basal expression of scopoletin, a preformed defense mechanism that contributes significantly to disease resistance against a biotrophic pathogen. Interestingly, the *MYB15* gene (At3g23250) is close to the map position of the highest LOD-scoring quantitative trait loci (SCT3) for scopoletin accumulation in Arabidopsis (Siwinska et al., 2014). Scopoletin is also a preformed defense mechanism in tobacco, contributing significantly to disease resistance against the necrotrophic pathogen *Alternaria alternata* (Sun et al., 2014). Although induced upon infection (~50 μg per gram of plant fresh weight; Sun et al., 2014), scopoletin is also expressed basally (~5 μg per gram of plant fresh weight; Sun et al., 2014) and thus cannot be considered a phytoalexin (by definition, a plant-formed antibiotic synthesized de novo after infection) (VanEtten et al., 1994). It is not known whether SG2-type R2R3-MYBs in tobacco are required for basal expression of scopoletin.

These studies suggest that SG2-type R2R3-MYBs are an invaluable resource for investigating preformed and inducible mechanisms of phenolic-based disease resistance in plants as well as the evolution of regulatory pathways in plant secondary metabolism.

Possible Evolutionary Relationship between SG2-Type and SG3-Type R2R3-MYBs

SG3-type R2R3-MYBs are involved in secondary cell wall formation in a number of angiosperm species. Phylogenetic analysis and sequence alignment suggest that SG2-type and SG3-type R2R3-MYBs are most closely related to one another among the

R2R3-MYB subgroups (Stracke et al., 2001; Supplemental Figure 4) and likely share a common evolutionary ancestor. The phenylpropanoid pathway is hypothesized to have evolved concurrently with the adaptation of plants to terrestrial life and the associated abiotic stresses (e.g., UV and drought) that accompany that change of environment (Weng and Chapple, 2010). By this logic, the regulation of stress-responsive pathways could precede the regulation of vascular development. In support of this hypothesis, MYB15 reportedly also reduces freezing tolerance (Agarwal et al., 2006) and improves salt and drought tolerance by enhancing abscisic acid sensitivity (Ding et al., 2009), although the mechanism(s) underlying these abiotic stress responses and their link(s) to phenylpropanoid metabolism remains unknown. Additional studies are needed to determine the ancestral function of the SG2- and SG3-type R2R3-MYBs and their relationship to each other.

Composition and Function of Defense-Induced Lignin

Arabidopsis has been the model system for studying the role of tryptophan-derived small molecules in plant innate immunity (Thomma et al., 1999; Bednarek et al., 2009; Clay et al., 2009; Rajniak et al. 2015), but comparatively little is known about the role of phenylalanine-derived small molecules and polymers in plant immunity. Fundamentally, little is known about how defense-induced lignin differs from its developmentally regulated counterpart in composition and physical properties. Our chemical and genetic data show that Arabidopsis defense-induced lignin is predominantly comprised of G-units and that the G-unit content of defense-induced lignin is mainly responsible for the MYB15-mediated basal resistance to a hemibiotrophic pathogen.

G-units are commonly found in condensed forms of lignin (Yelle et al., 2008). Ideally, for defense-induced lignin to be less prone to degradation by microbial enzymes, the lignin structure should be comprised of phenylcoumaran, resinol, and dibenzodioxocin linkages. G-units can form the widest range of linkages due to a methoxy group on the phenyl head, whereas S-units are sterically hindered from making some of the more complex linkages found in G-lignin (e.g., phenylcoumaran and dibenzodioxocin linkages) due to the presence of a second methoxy group on the phenyl head (Yelle et al., 2008).

Although H-lignin units are present in trace quantities in unelicited and flg22-elicited Arabidopsis seedlings, they are the major constituents of defense-induced lignin in spruce (Lange et al., 1995), a gymnosperm species. H-units form the simplest and most flexible linkages. For this reason, it remains unclear whether defense-induced lignin in gymnosperms would have the same function as defense-induced lignin in angiosperms.

Regulatory Relationship between Branches of Phenylpropanoid Metabolism

The scopoletin-deficient *f6'h1* mutant could contain additional defects in the defense-induced synthesis of G-lignin or MYB15-induced synthesis of soluble phenolics, which would account for the discrepancy between the mutant and chemical data. This was shown to be the case for the S-lignin-deficient *fah1-2* mutant, which is also affected in the synthesis of HCAEs and anthocyanins (Anderson et al., 2015). Similarly, the *f6'h1* mutant is also affected in the synthesis of HCAEs 1-sinapoylglucose and 1,2-disinapoylglucose in the absence of flg22 elicitation (Figure 6D), whereas *f6'h1* and the scopoletin transporter-deficient *pdr9/abcg37* mutant (Fourcroy et al., 2014) produce a wild-type level of flg22-induced lignin response (Supplemental Figure 2B). Since MYB15-induced synthesis of HCAEs is additionally affected in the *f6'h1* mutant, it remains unclear whether scopoletin deficiency is mainly responsible for the increased susceptibility observed in the *f6'h1* mutant.

A recent quantitative trait loci mapping study for scopoletin biosynthesis identified monolignol pathway genes *HCT* and *COMT* as possible candidate regulators of scopoletin biosynthesis (Siwinska et al., 2014), lending further support to the existence of a complex regulatory relationship between the monolignol, HCAE, and scopoletin biosynthetic pathways.

Regulatory Relationship between Lignin, Growth, and Defense

MYB15 and MYB58/63 are functionally related; that is, they both activate lignin biosynthesis (Zhou et al., 2009; Figures 1 to 4) and contribute to inflorescence growth (Supplemental Figure 5). However, only MYB15 contributes to disease resistance to a hemibiotrophic pathogen (Figure 5). These results suggest a functional distinction between defense-induced lignification and vascular cell wall lignification.

Downregulation or knockout of monolignol pathway genes hydroxycinnamoyl CoA:shikimate hydroxycinnamoyl transferase (HCT), *p*-coumaroyl shikimate 3′-hydroxylase (C3′H), caffeoyl shikimate esterase (CSE), and CCR (Supplemental Figure 1) result in severe defects in plant growth and development (Elkind et al., 1990; Piquemal et al., 1998; Pinçon et al., 2001; Franke et al., 2002, O'Connell et al., 2002; Hoffmann et al., 2004; Rohde et al., 2004; Reddy et al., 2005; Leplé et al., 2007; Besseau et al., 2007; Li et al., 2010; Zhou et al., 2010; Gallego-Giraldo et al., 2011a; Vanholme et al., 2013). These growth defects were often accompanied by constitutive defense responses and increased immunity to (hemi)biotrophic pathogens (Gallego- Giraldo et al., 2011a; Lee et al., 2011). High levels of SA can also repress plant growth (Rivas-San Vicente and Plasencia, 2011) and are thought to be responsible for the growth defects in HCT-downregulated Arabidopsis plants (Gallego-Giraldo et al., 2011b). By contrast, C3′H-defective Arabidopsis plants accumulate wild-type levels of SA, and its growth defects are caused instead by stress-induced transcriptional repression of growth-promoting genes by the transcriptional coregulator Mediator (Bonawitz et al., 2014). MYB15 also plays a role in the complex regulatory relationship between lignin, growth, and defense, and further research is needed to determine the extent of MYB15's involvement, if any, in the growth defects observed in lignin biosynthetic mutants.

METHODS

Plant Materials and Growth Conditions

For transcriptional and metabolomics analyses, surface-sterilized seeds of *Arabidopsis thaliana* accession Columbia-0 (Col-0) were sown in 12-well microtiter plates sealed with Micropore tape (3M), each well containing ~10

to 15 seeds and 1 mL of filter-sterilized 1× Murashige and Skoog (MS; Murashige and Skoog, 1962) media (pH 5.7–5.8) (4.43 g/L MS basal medium with vitamins [Phytotechnology Laboratories], 0.05% MES hydrate, and 0.5% sucrose). For lignin quantification and ChIP, seeds were sown in 6-well microtiter dishes, each well containing ~30 to 45 seeds and 3 mL of MS media. Media were exchanged for fresh media on day 7. Microtiter plates were placed on grid-like shelves over water trays on a Floralight cart, and plants were grown under long-day conditions (16-h light [70-80 $\mu E\ m^{-2}\ s^{-1}$ light intensity], 21°C, and 60% humidity). For bacterial infection experiments, Arabidopsis were grown on soil (Fafard Growing Mix 2; Sun Gro Horticulture) under day-neutral conditions (12-h light [50, dawn/dusk, and 100, midday, $\mu E\ m^{-2}\ s^{-1}$ light intensity], 22°C day/18°C night, and 60% humidity) for 4 weeks. For inflorescence growth experiments, plants (five per pot) were grown first under day-neutral conditions (12-h light) for 4 weeks and then transferred to long-day conditions (16-h light [100 $\mu E\ m^{-2}\ s^{-1}$ light intensity]) to allow the development of a single tall inflorescent stem. The following homozygous Col-0 T-DNA insertion lines and mutants were obtained from the Arabidopsis Biological Resource Center: *aact1-1* (SALK_097380), *ccr1-6* (GABI_622C01), *cse-2* (SALK_023077), *f6'h1-1* (SALK_132418), *fah1-2/f5 h* (CS6172), *fls2* (SAIL_691_C4), *myb13* (GABI_274B08), *myb14* (SALK_018565), *myb15-1* (SALK_151976), *myb15-2* (SK2722), *myb58* (GABI_532E09), *myb63* (GABI_762D10), *omt1-2/comt* (SALK_135290), *pal1-3* (SALK_096474), *pdr9/abcg37* (SALK_035704), and *ugt84A1* (SALK_129336). The T-DNA insertion in *myb15-1* is after amino acid 173; the T-DNA insertion in *myb15-2* is in the R3-MYB domain after amino acid 87.

Plant Binary Vector Construction and Transformation

To generate the *35S:MYB15* DNA construct, the *MYB15* coding sequence was PCR-amplified from genomic DNA using the primers MYB15gXhoF (5′-AACTCGAGACTATGTTGCCAATAATCAA-3′) and MYB15gXbaR (5′-TTCCCGGGGAGCCCGGCTAAGAGATC-3′) and subcloned into the *Xho*I/*Stu*I sites of pJIM19(Bar), a pBIN19 derivative that contains a BASTA resistance marker and a MCS downstream of the 35SCaMV promoter. To generate the *DEX:MYB15* construct, the *MYB15* coding sequence was PCR-amplified using the primers MYB15gXhoF and MYB15gStuR (5′-AAGGCCTGAGCCCGGCTAAGAGATC-3′) and subcloned into the *Xho*I/*Stu*I sites of pTA7002 vector (Aoyama and Chua, 1997), modified to contain six tandem copies of the c-Myc epitope downstream of the *Stu*I site. The *35S:MYB15* and *DEX:MYB15* constructs were introduced into Arabidopsis *myb15-1* plants via the *Agrobacterium tumefaciens*-mediated floral dip method (Clough and Bent, 1998), and transformants were selected on agar media containing 15 μg/mL BASTA (glufosinate-ammonium; Riedel-de Haen) or 15 μg/mL hygromycin B (Invitrogen), respectively.

Lignin Analysis by Phloroglucinol-HCl Staining

Lignin staining was performed as described previously (Adams-Phillips et al., 2010) with some modifications. Briefly, 9-d-old seedlings in MS media were elicited with 1 μM flg22 (QRLSTGSRINSAKDDAAGLQIA; Genscript), 1 μM elf26 (ac-SKEKFERTKPHVNVGTIGHVDHGKTT; Genscript), or water for 48 or 72 h. Elicited plant tissues were then fixed with (3:1) 95% (v/v) ethanol to glacial acetic acid under brief vacuum and then on a shaking platform with several changes of fixative for several hours until tissues appeared slightly translucent. Fixative was then exchanged for 75% ethanol for 30 min, then 50% ethanol for 30 min, and then water overnight to rehydrate seedlings. Seedlings were stained in phloroglucinol-HCl solution (1% [w/v] phloroglucinol [Sigma-Aldrich] in 50% [v/v] concentrated HCl) for 5 min prior to being photographed.

Lignin Analysis by Acetyl Bromide Method

Microscale lignin quantification was performed as previously described (Moreira-Vilar et al., 2014) with modifications. Briefly, 10-d-old Arabidopsis seedlings or 10-cm cuttings of mature rice leaves from 4-month-old plants were snap-frozen in liquid nitrogen, lyophilized, and then homogenized, using a 5-mm diameter stainless steel bead and a ball mill (25 Hz for 2 min). Samples were extracted with the following solvents in an ultrasonic bath for 15 min each: 2× 1-mL methanol, 2× 1× PBS containing 0.1% (v/v) Tween 20, 2× 1-mL 95% ethanol, 2× 1-mL (1:1) chloroform to methanol, and 2× 1-mL acetone. After each extraction, samples were centrifuged at 16,000*g* for 10 min and the supernatant discarded. The remaining CWR was dried at 50°C in a GeneVac EZ-2Plus (Genevac), homogenized in a ball mill with 10 to 15 1-mm zirconia beads for 10 min at 25 Hz, dissolved in 1.5 mL of 25% (v/v) acetyl bromide (Sigma-Aldrich) in glacial acetic acid, and heated at 50°C for 2 h, with occasional shaking. Samples were cooled on ice. The sample (125 μL) was transferred to a centrifuge tube containing 250 μL of (1:9) 5 M hydroxylamine HCl (Sigma-Aldrich) to 2 M NaOH and 500 μL of glacial acetic acid. Five hundred microliters of the mix was transferred to a 1-cm diameter glass cuvette for absorbance measurement at 280 nm. Lignin content was calculated using the extinction coefficient 23.35 mg/cm/L for Arabidopsis (Chang et al., 2008) using Beer's law ($A = \varepsilon lc$).

Lignin Analysis by DFRC Method

The DFRC lignin analysis was performed essentially as previously reported (Lu and Ralph, 1998). Briefly, extractive-free cell wall samples were dissolved in acetyl bromide/acetic acid solution, containing 4,4′-ethylidenebisphenol as an internal standard. The reaction products were dried down using nitrogen gas, dissolved in dioxane/acetic acid/water (5/4/1, v/v/v), reacted with Zn dust, purified with C-18 SPE columns (Supelco), and acetylated with pyridine/acetic anhydride (2/3, v/v). The lignin derivatives were analyzed by an Agilent 5977 Series gas chromatography-mass spectrometry system. The quantification of coniferyl alcohol peracetate, sinapyl alcohol peracetate, and 4,4′-ethylidenebisphenol peracetate was based on peak integration of the extracted ion chromatograms monitoring the *m/z* of 222, 252, and 256, respectively. The response factors for G and S monolignol derivatives relative to the internal standard were calibrated based on pure standards.

qPCR Analysis

Total RNA was extracted from snap-frozen 10-d-old seedlings using TRIzol reagent (Invitrogen) according to the manufacturer's instructions. Total RNA (2.5 μg) was reverse-transcribed with 3.75 μM random hexamers (Qiagen) and 20 units of ProtoScript II (New England Biolabs) according to the manufacturer's instructions. The resulting cDNA:RNA hybrids were treated with 10 units of DNase I (Roche) for 30 min at 37°C and purified on PCR clean-up columns (Macherey-Nagel). qPCR was performed with Kapa SYBR Fast qPCR master mix (Kapa Biosystems) and CFX96 real-time PCR machine (Bio-Rad). The thermal cycling program was as follows: 95°C for 3 min; 45 cycles of 95°C for 15 s and 53°C for 30 s; a cycle of 95°C for 1 min, 53°C for 1 min, and 70°C for 10 s; and 50 cycles of 0.5°C increments for 10 s. Four biological replicates of control and experimental samples and three technical replicates per biological replicate were performed on the same 96-well PCR plate. Average of the three Ct values per biological replicate was converted to difference in Ct value relative to that of control sample. The Pfaffl method (Pfaffl, 2001) and calculated primer efficiencies were used to determine the relative fold induction of target gene transcript over *eIF4A1* (AT3G13920) housekeeping gene transcript for each biological replicate. Primer sequences and efficiencies are listed in Supplemental Table 2.

ChIP

ChIP was performed as previously described by Fiil et al. (2008) and Roccaro and Somssich (2011) with some modifications. Approximately 210 8-d-old seedlings were treated with mock solution (DMSO) or 20 μM Dex for 4 h, rinsed twice with deionized water, immersed in 1% (v/v)

formaldehyde solution, and vacuum-infiltrated for 10 min. After a 5-min quenching step with 2 M glycine, seedlings were washed three times with deionized water, vacuum-dried, and snap-frozen with liquid nitrogen. Following frozen homogenization with a mortar and pestle, the homogenate was filtered once through a 70-μm mesh (Carolina Biological) and a 0.45-μm filter (EMD Millipore). Filtered homogenate was then washed once in extraction buffer 2 prior to sucrose centrifugation. Following nuclear extraction, samples were sonicated in a Covaris S2 sonicator (Covaris) using 10% duty, 7% intensity, and 200 cycles per burst for a total time of 12 min. Nuclei lysis and ChIP dilution buffers were made according to Fiil et al. (2008). ChIP was performed using EZview Red Anti-c-Myc Affinity Gel (Sigma-Aldrich) pretreated with 0.1% (w/v) nonfat milk in 1× PBS and 0.1% (w/v) sheared salmon sperm DNA (Invitrogen). Following de-cross-linking, DNA samples were phenol-chloroform-extracted and diluted to a concentration of 40 ng/μL prior to PCR. Primer sequences are listed in Supplemental Table 1. Two microliters of immunoprecipitated DNA and 2.5 μM $MgCl_2$ were used in ChIP-PCR with the exception of the *CAD5p1* primers, which required 4 μM $MgCl_2$. PCR conditions were as follows: 40 cycles, 94°C for 15 s, 53°C for 15 s, and 72°C for 15 s. PCR product intensities were measured using NIH ImageJ software. In cases where the PCR product is undetectable, the number "10" was arbitrarily used in lieu of "0" to calculate fold enrichment.

Extraction and LC-MS/MS Analysis of Soluble Phenolics

Ten-day-old seedlings were snap-frozen in liquid nitrogen, lyophilized, weighed, and homogenized using a 5-mm stainless steel bead and a ball mill (25 Hz for 4 min). The homogenate was then extracted with 1 mL of methanol containing 1 μL of 20 μg/mL daidzein (internal standard; Sigma-Aldrich) per milligram sample dry weight. The extract was sonicated for 30 min, centrifuged at 13,200*g* for 15 min to remove supernatant, and then the extraction was repeated with pure methanol. Combined supernatants for each sample were then evaporated at ambient temperature in a GeneVac EZ-2Plus, resuspended in 250 μL of 50% methanol, and filtered using a 0.45 μm PVDF filter plate (EMD Millipore). Samples were separated by reversed-phase chromatography on an Agilent 1290 UHPLC using a 1.7-μm, 2.1 × 100-mm Kinetex C18 column (Phenomenex); volume injected was 5 μL. The following 40-min gradient in 0.1% formic acid was used for metabolomics analysis (percentages indicate acetonitrile concentration): 0 to 40 min, 0 to 100%. A coupled Agilent 6550A QTOF mass spectrometer was used to collect MS data in positive ion mode (parameters: mass range, 100–1500 *m/z*; drying gas, 250°C, 14 L/min; nebulizer, 50 psig; capillary, 4000 V; fragmentor, 100 V; skimmer, 65 V; octupole 1 RF; Vpp, 570 V; 1000 ms per spectrum). High-resolution mass spectrometry data were analyzed using the Agilent MassHunter Qualitative Analysis program. Extracted ion chromatogram data were derived from raw data files using MassHunter Qualitative software, using a 25-ppm window centered on the exact *m/z* value with automated integration of the peak area.

Extraction and HPLC-FLD Analysis of Total Scopoletin

Samples were lyophilized and homogenized as described above and then extracted with 750 μL of methanol containing 1 μL of 20 ng/mL 4-methylumbelliferone (4-MeU; internal standard; Sigma-Aldrich) per milligram sample dry weight. The extract was sonicated for 10 min, centrifuged for 10 min at maximum speed to remove supernatant, and then the extraction was repeated with pure methanol. The extracts were then combined and evaporated using a GeneVac EZ-2Plus. To hydrolyze scopoletin glycosides present in the samples to free scopoletin, extracts were resuspended in 4 M HCl and heated at 80°C for 1 h. The samples were then extracted twice with (1:1) cyclohexane to ethyl acetate. Sixty microliters of 0.2 N NaOAc (pH 5.5) was added to the combined organic fractions, and samples were sonicated for 5 min, centrifuged for 5 min, evaporated to 50 μL, resuspended in 200 μL of 50% methanol, and filtered using a 0.45-μm filter plate. Samples were separated by reversed-phase chromatography on an Ultimate 3000 HPLC system (Dionex), using a 4-μm, 3 × 150-mm Phenomenex Polar RP-80 column; volume injected was 20 μL. The following 25-min gradient in 0.1% formic acid was used for HPLC analysis (percentages indicate acetonitrile concentration): 0 to 5 min, 4.5 to 9%; 5 to 15 min, 9 to 22.5%; 15 to 23 min, 22.5 to 63%; 23 to 25 min, 63 to 90%. A coupled FLD-3100 detector (Dionex) collected fluorescent data at 365/462 nm (excitation/emission) for scopoletin and 340/420 nm (excitation/emission) for 4-MeU. A standard curve of scopoletin standards (Sigma-Aldrich) and percent recovery (estimated by the quantification of the internal standard 4-MeU) were used for absolute quantification of total scopoletin amounts.

HPLC-DAD Analysis of 1-Sinapoylglucose and 1,2-Disinapoylglucose

Extraction is described in LC-MS/MS section above. Samples were separated using the same system described above with the following modifications: 25-min gradient in 0.1% formic acid (percentages indicate acetonitrile concentration): 0 to 10 min, 9 to 18%; 10 to 20 min, 18 to 36% B; 20 to 22 min, 36 to 100%, 22 to 25 min at 100%. A coupled DAD-3000RS diode array detector (Dionex) collected UV absorption spectra in the range of 210 to 330 nm for identification and quantification of sinapate esters. Integrated areas of 1-sinapoylglucose, 1,2-disinapoylglucose and daidzein (internal standard) peaks in the UV chromatographs at 330 nm were used for relative quantification.

Bacterial Infection Assays

Pseudomonas syringae pv *tomato* DC3000 (*Pto* DC3000) was used for bacterial infections. *Pto* DC3000 was grown in Luria-Bertani medium and 25 μg/mL rifampicin (Sigma-Aldrich) overnight, washed in sterile water twice, and resuspended in water to the desired OD_{600}. Hydroponically grown 8-d-old seedlings were pretreated with 1 μM flg22 or water for 6 h prior to treatment with the bacterial inoculum (OD_{600} = 0.001) for 24 h. Adult leaves of 5-week-old plants were surface-inoculated with the bacterial inoculum (OD_{600} = 0.002 or 10^6 colony-forming units [CFU]/cm^2 leaf area) in the presence of 0.0075% Silwet L-77 (Phytotechnology Laboratories) for 15 s and incubated in 0.8% (w/v) tissue culture agar plates for 3 to 4 d. Infected seedlings and leaves were surface-sterilized in 70% ethanol for 10 s, washed in sterile water, and dried on paper towels, and the bacteria were extracted into water, using an 8-mm stainless steel bead and a ball mill (25 Hz for 3 min). Serial dilutions of the extracted bacteria were plated on Luria-Bertani agar plates for CFU counting. For the protection experiment, each leaf was preinfiltrated with ~100 μL solution of 500 nM phenolic compounds and 1 μM flg22 for 24 h prior to infiltration with the bacterial inoculum (OD_{600} = 0.0002 or 10^5 CFU/cm^2 leaf area).

Accession Numbers

Sequence data from this article can be found in the Arabidopsis Genome Initiative or GenBank/EMBL databases under the following accession numbers: OAP02219.1 (AtMYB15), OAP12852.1 (AtMYB13), NP_180676.1 (AtMYB14), KF767453 (EjMYB1 cDNA), AID56313 (EjMYB1), NP_001268132.1 (VvMYB14), AHA83524.1 (VvMYB15), NP_173098.1 (AtMYB58), NP_178039.1 (AtMYB63), P20024.1 (ZmMYB19/Zm1), and XP_002452709.1 (SbMYB60).

Supplemental Data

Supplemental Figure 1. Genes and products of the monolignol and branch pathways in Arabidopsis.

Supplemental Figure 2. *MYB15* is required for defense-inducible lignin response.

Supplemental Figure 3. Amino acid sequence alignment of MYB15 (SG2-type) and MYB58 (SG3-type) homologs.

Supplemental Figure 4. Putative evolutionary relationships among Arabidopsis R2R3-MYB proteins.

Supplemental Figure 5. Growth phenotypes of SG2-type and SG3-type R2R3-MYB transcription factor mutants.

Supplemental Figure 6. MYB15-myc protein expression.

Supplemental Figure 7. MYB15 increases the synthesis of soluble phenolics independently of flg22.

Supplemental Figure 8. *MYB13* and *MYB14* genes and proteins.

Supplemental Table 1. ChIP-PCR primer sequences and AC-like *cis*-elements.

Supplemental Table 2. qPCR primer sequences and efficiencies.

Supplemental File 1. Text file of alignment used for phylogenetic analysis in Supplemental Figure 3.

Supplemental File 2. Text file of alignment used for phylogenetic analysis in Supplemental Figure 4.

ACKNOWLEDGMENTS

We thank F.M. Ausubel and members of the Clay laboratory for comments on the manuscript. We thank J. Crawford and E. Trautman for advice on LC-MS/MS data analysis. This work was supported by NIH Genetics Training Grant T32 GM007499 (to W.R.C. and A.M.), by an Elsevier/Phytochemistry Young Investigator Award (to N.K.C.), by Pew Scholar Program in the Biomedical Sciences (to J.K.W), and by the Searle Scholars Program (to J.K.W.).

AUTHOR CONTRIBUTIONS

F.-S.L. and J.-K.W. performed DFRC lignin analysis. A.M. performed AcBr lignin analysis of *DEX:MYB15* lines. W.R.C. and A.M. performed scopoletin analysis. W.R.C. and N.K.C. performed ChIP-PCR and pathogen assays. W.R.C. performed all other experiments. W.R.C. and N.K.C. interpreted the results and wrote the article.

Received December 20, 2016; revised June 22, 2017; accepted July 17, 2017; published July 21, 2017.

REFERENCES

Adams-Phillips, L., Briggs, A.G., and Bent, A.F. (2010). Disruption of poly(ADP-ribosyl)ation mechanisms alters responses of Arabidopsis to biotic stress. Plant Physiol. **152:** 267–280.

Agarwal, M., Hao, Y., Kapoor, A., Dong, C.-H., Fujii, H., Zheng, X., and Zhu, J.-K. (2006). A R2R3 type MYB transcription factor is involved in the cold regulation of CBF genes and in acquired freezing tolerance. J. Biol. Chem. **281:** 37636–37645.

Anderson, N.A., Bonawitz, N.D., Nyffeler, K., and Chapple, C. (2015). Loss of FERULATE 5-HYDROXYLASE leads to Mediator-dependent inhibition of soluble phenylpropanoid biosynthesis in Arabidopsis. Plant Physiol. **169:** 1557–1567.

Aoyama, T., and Chua, N.H. (1997). A glucocorticoid-mediated transcriptional induction system in transgenic plants. Plant J. **11:** 605–612.

Baayen, R.P., Ouellette, G.B., and Rioux, D. (1996). Compartmentalization of decay in carnations resistant to *Fusarium oxysporum* f. sp. *dianthi.* Phytopathology **86:** 1018–1031.

Bednarek, P., Pislewska-Bednarek, M., Svatos, A., Schneider, B., Doubsky, J., Mansurova, M., Humphry, M., Consonni, C., Panstruga, R., Sanchez-Vallet, A., Molina, A., and Schulze-Lefert, P. (2009). A glucosinolate metabolism pathway in living plant cells mediates broad-spectrum antifungal defense. Science **323:** 101–106.

Besseau, S., Hoffmann, L., Geoffroy, P., Lapierre, C., Pollet, B., and Legrand, M. (2007). Flavonoid accumulation in *Arabidopsis* repressed in lignin synthesis affects auxin transport and plant growth. Plant Cell **19:** 148–162.

Boerjan, W., Ralph, J., and Baucher, M. (2003). Lignin biosynthesis. Annu. Rev. Plant Biol. **54:** 519–546.

Boller, T., and Felix, G. (2009). A renaissance of elicitors: perception of microbe-associated molecular patterns and danger signals by pattern-recognition receptors. Annu. Rev. Plant Biol. **60:** 379–406.

Bonawitz, N.D., and Chapple, C. (2010). The genetics of lignin biosynthesis: connecting genotype to phenotype. Annu. Rev. Genet. **44:** 337–363.

Bonawitz, N.D., Kim, J.I., Tobimatsu, Y., Ciesielski, P.N., Anderson, N.A., Ximenes, E., Maeda, J., Ralph, J., Donohoe, B.S., Ladisch, M., and Chapple, C. (2014). Disruption of Mediator rescues the stunted growth of a lignin-deficient *Arabidopsis* mutant. Nature **509:** 376–380.

Bhuiyan, N.H., Selvaraj, G., Wei, Y., and King, J. (2009). Gene expression profiling and silencing reveal that monolignol biosynthesis plays a critical role in penetration defence in wheat against powdery mildew invasion. J. Exp. Bot. **60:** 509–521.

Chang, X.F., Chandra, R., Berleth, T., and Beatson, R.P. (2008). Rapid, microscale, acetyl bromide-based method for high-throughput determination of lignin content in *Arabidopsis thaliana*. J. Agric. Food Chem. **56:** 6825–6834.

Chen, F., and Dixon, R.A. (2007). Lignin modification improves fermentable sugar yields for biofuel production. Nat. Biotechnol. **25:** 759–761.

Chen, H.C., et al. (2014). Systems biology of lignin biosynthesis in *Populus trichocarpa*: heteromeric 4-coumaric acid:coenzyme A ligase protein complex formation, regulation, and numerical modeling. Plant Cell **26:** 876–893.

Chen, Y., Zhang, X., Wu, W., Chen, Z., Gu, H., and Qu, L.-J. (2006a). Overexpression of the wounding-responsive gene *AtMYB15* activates the shikimate pathway in *Arabidopsis.* J. Integr. Plant Biol. **48:** 1084–1095.

Clay, N.K., Adio, A.M., Denoux, C., Jander, G., and Ausubel, F.M. (2009). Glucosinolate metabolites required for an Arabidopsis innate immune response. Science **323:** 95–101.

Clifford, M.N. (1974). Specificity of acidic phloroglucinol reagents. J. Chromatogr. A **94:** 321–324.

Clough, S.J., and Bent, A.F. (1998). Floral dip: a simplified method for *Agrobacterium*-mediated transformation of *Arabidopsis thaliana.* Plant J. **16:** 735–743.

Denoux, C., Galletti, R., Mammarella, N., Gopalan, S., Werck, D., De Lorenzo, G., Ferrari, S., Ausubel, F.M., and Dewdney, J. (2008). Activation of defense response pathways by OGs and Flg22 elicitors in Arabidopsis seedlings. Mol. Plant **1:** 423–445.

Dien, B.S., Sarath, G., Pedersen, J.F., Sattler, S.E., Chen, H., Funnell-Harris, D.L., Nichols, N.N., and Cotta, M.A. (2009). Improved sugar conversion and ethanol yield for forage sorghum (*Sorghum bicolor* L. Moench) lines with reduced lignin contents. BioEnergy Res. **2:** 153–164.

Ding, Z., Li, S., An, X., Liu, X., Qin, H., and Wang, D. (2009). Transgenic expression of MYB15 confers enhanced sensitivity to abscisic acid and improved drought tolerance in *Arabidopsis thaliana*. J. Genet. Genomics **36:** 17–29.

Dong, H.-P., Peng, J., Bao, Z., Meng, X., Bonasera, J.M., Chen, G., Beer, S.V., and Dong, H. (2004). Downstream divergence of the ethylene signaling pathway for harpin-stimulated Arabidopsis growth and insect defense. Plant Physiol. **136:** 3628–3638.

Doster, M.A., and Bostock, R.M. (1988). Quantification of lignin formation in almond bark in response to wounding and infection by *Phytophthora* species. Phytopathology **78:** 473–477.

Elkind, Y., Edwards, R., Mavandad, M., Hedrick, S.A., Ribak, O., Dixon, R.A., and Lamb, C.J. (1990). Abnormal plant development and down-regulation of phenylpropanoid biosynthesis in transgenic tobacco containing a heterologous phenylalanine ammonia-lyase gene. Proc. Natl. Acad. Sci. USA **87:** 9057–9061.

Ferrer, J.L., Austin, M.B., Stewart, C., Jr., and Noel, J.P. (2008). Structure and function of enzymes involved in the biosynthesis of phenylpropanoids. Plant Physiol. Biochem. **46:** 356–370.

Fiil, B.K., Qiu, J.L., Petersen, K., Petersen, M., and Mundy, J. (2008). Coimmunoprecipitation (co-IP) of nuclear proteins and chromatin immunoprecipitation (ChIP) from Arabidopsis. Cold Spring Harb. Protoc. **3:** 10.1101/pdb.prot5049.

Franke, R., Hemm, M.R., Denault, J.W., Ruegger, M.O., Humphreys, J.M., and Chapple, C. (2002). Changes in secondary metabolism and deposition of an unusual lignin in the ref8 mutant of Arabidopsis. Plant J. **30:** 47–59.

Franken, P., Schrell, S., Peterson, P.A., Saedler, H., and Wienand, U. (1994). Molecular analysis of protein domain function encoded by the *myb*-homologous maize genes *C1, Zm 1* and *Zm 38.* Plant J. **6:** 21–30.

Fourcroy, P., Sisó-Terraza, P., Sudre, D., Savirón, M., Reyt, G., Gaymard, F., Abadía, A., Abadía, J., Alvarez-Fernández, A., and Briat, J.F. (2014). Involvement of the ABCG37 transporter in secretion of scopoletin and derivatives by Arabidopsis roots in response to iron deficiency. New Phytol. **201:** 155–167.

Gallego-Giraldo, L., Escamilla-Trevino, L., Jackson, L.A., and Dixon, R.A. (2011a). Salicylic acid mediates the reduced growth of lignin down-regulated plants. Proc. Natl. Acad. Sci. USA **108:** 20814–20819.

Gallego-Giraldo, L., Jikumaru, Y., Kamiya, Y., Tang, Y., and Dixon, R.A. (2011b). Selective lignin downregulation leads to constitutive defense response expression in alfalfa (*Medicago sativa* L.). New Phytol. **190:** 627–639.

Gómez-Gómez, L., and Boller, T. (2000). FLS2: an LRR receptor-like kinase involved in the perception of the bacterial elicitor flagellin in *Arabidopsis.* Mol. Cell **5:** 1003–1011.

Gómez-Gómez, L., and Boller, T. (2002). Flagellin perception: a paradigm for innate immunity. Trends Plant Sci. **7:** 251–256.

Goujon, T., Sibout, R., Pollet, B., Maba, B., Nussaume, L., Bechtold, N., Lu, F., Ralph, J., Mila, I., Barrière, Y., Lapierre, C., and Jouanin, L. (2003). A new *Arabidopsis thaliana* mutant deficient in the expression of *O*-methyltransferase impacts lignins and sinapoyl esters. Plant Mol. Biol. **51:** 973–989.

Hammerschmidt, R., Bonnen, A.M., Bergstrom, G.C., and Baker, K.K. (1985). Association of epidermal lignification with nonhost resistance of cucurbits to fungi. Can. J. Bot. **63:** 2393–2398.

Hatton, D., Sablowski, R., Yung, M.-H., Smith, C., Schuch, W., and Bevan, M. (1995). Two classes of cis sequences contribute to tissue-specific expression of a *PAL2* promoter in transgenic tobacco. Plant J. **7:** 859–876.

Hoffmann, L., Besseau, S., Geoffroy, P., Ritzenthaler, C., Meyer, D., Lapierre, C., Pollet, B., and Legrand, M. (2004). Silencing of hydroxycinnamoyl-coenzyme A shikimate/quinate hydroxycinnamoyltransferase affects phenylpropanoid biosynthesis. Plant Cell **16:** 1446–1465.

Höll, J., Vannozzi, A., Czemmel, S., D'Onofrio, C., Walker, A.R., Rausch, T., Lucchin, M., Boss, P.K., Dry, I.B., and Bogs, J. (2013). The R2R3-MYB transcription factors MYB14 and MYB15 regulate stilbene biosynthesis in *Vitis vinifera.* Plant Cell **25:** 4135–4149.

Huang, J., Gu, M., Lai, Z., Fan, B., Shi, K., Zhou, Y.H., Yu, J.Q., and Chen, Z. (2010). Functional analysis of the *Arabidopsis PAL* gene family in plant growth, development, and response to environmental stress. Plant Physiol. **153:** 1526–1538.

Jones, J.D.G., and Dangl, J.L. (2006). The plant immune system. Nature **444:** 323–329.

Jones, L., Ennos, A.R., and Turner, S.R. (2001). Cloning and characterization of *irregular xylem4* (*irx4*): a severely lignin-deficient mutant of *Arabidopsis.* Plant J. **26:** 205–216.

Kai, K., Shimizu, B., Mizutani, M., Watanabe, K., and Sakata, K. (2006). Accumulation of coumarins in *Arabidopsis thaliana.* Phytochemistry **67:** 379–386.

Kai, K., Mizutani, M., Kawamura, N., Yamamoto, R., Tamai, M., Yamaguchi, H., Sakata, K., and Shimizu, B. (2008). Scopoletin is biosynthesized via ortho-hydroxylation of feruloyl CoA by a 2-oxoglutarate-dependent dioxygenase in *Arabidopsis thaliana.* Plant J. **55:** 989–999.

Kaku, H., Nishizawa, Y., Ishii-Minami, N., Akimoto-Tomiyama, C., Dohmae, N., Takio, K., Minami, E., and Shibuya, N. (2006). Plant cells recognize chitin fragments for defense signaling through a plasma membrane receptor. Proc. Natl. Acad. Sci. USA **103:** 11086–11091.

Kawasaki, T., Koita, H., Nakatsubo, T., Hasegawa, K., Wakabayashi, K., Takahashi, H., Umemura, K., Umezawa, T., and Shimamoto, K. (2006). Cinnamoyl-CoA reductase, a key enzyme in lignin biosynthesis, is an effector of small GTPase Rac in defense signaling in rice. Proc. Natl. Acad. Sci. USA **103:** 230–235.

Kishi-Kaboshi, M., Okada, K., Kurimoto, L., Murakami, S., Umezawa, T., Shibuya, N., Yamane, H., Miyao, A., Takatsuji, H., Takahashi, A., and Hirochika, H. (2010). A rice fungal MAMP-responsive MAPK cascade regulates metabolic flow to antimicrobial metabolite synthesis. Plant J. **63:** 599–612.

König, S., Feussner, K., Kaever, A., Landesfeind, M., Thurow, C., Karlovsky, P., Gatz, C., Polle, A., and Feussner, I. (2014). Soluble phenylpropanoids are involved in the defense response of Arabidopsis against *Verticillium longisporum.* New Phytol. **202:** 823–837.

Kunze, G., Zipfel, C., Robatzek, S., Niehaus, K., Boller, T., and Felix, G. (2004). The N terminus of bacterial elongation factor *Tu* elicits innate immunity in Arabidopsis plants. Plant Cell **16:** 3496–3507.

Lange, B.M., Lapierre, C., and Sandermann, H., Jr. (1995). Elicitor-induced spruce stress lignin: structural similarity to early developmental lignins. Plant Physiol. **108:** 1277–1287.

Lawton, M.A., and Lamb, C.J. (1987). Transcriptional activation of plant defense genes by fungal elicitor, wounding, and infection. Mol. Cell. Biol. **7:** 335–341.

Lee, S., Sharm, Y., Lee, T.K., Chang, M., and Davis, K.R. (2001). Lignification induced by pseudomonads harboring avirulent genes on Arabidopsis. Mol. Cells **12:** 25–31.

Lee, Y., Chen, F., Gallego-Giraldo, L., Dixon, R.A., and Voit, E.O. (2011). Integrative analysis of transgenic alfalfa (*Medicago sativa* L.) suggests new metabolic control mechanisms for monolignol biosynthesis. PLOS Comput. Biol. **7:** e1002047.

Leplé, J.C., et al. (2007). Downregulation of cinnamoyl-coenzyme A reductase in poplar: multiple-level phenotyping reveals effects on cell wall polymer metabolism and structure. Plant Cell **19:** 3669–3691.

Lesney, M.S. (1989). Growth responses and lignin production in cell suspension of *Pinus elliottii* 'elicited' by chitin, chitosan or mycelium of *Cronartium quercum* f. sp. *fusiforme*. Plant Cell Tiss. Org. Cult. **19:** 23–31.

Li, X., Bonawitz, N.D., Weng, J.K., and Chapple, C. (2010). The growth reduction associated with repressed lignin biosynthesis in *Arabidopsis thaliana* is independent of flavonoids. Plant Cell **22:** 1620–1632.

Li, X., Weng, J.K., and Chapple, C. (2008). Improvement of biomass through lignin modification. Plant J. **54:** 569–581.

Lim, E.K., Li, Y., Parr, A., Jackson, R., Ashford, D.A., and Bowles, D.J. (2001). Identification of glucosyltransferase genes involved in sinapate metabolism and lignin synthesis in *Arabidopsis.* J. Biol. Chem. **276:** 4344–4349.

Liu, R., Lü, B., Wang, X., Zhang, C., Zhang, S., Qian, J., Chen, L., Shi, H., and Dong, H. (2010). Thirty-seven transcription factor genes differentially respond to a harpin protein and affect resistance to the green peach aphid in *Arabidopsis.* J. Biosci. **35:** 435–450.

Lu, F., and Ralph, J. (1998). The DFRC method for lignin analysis. 2. Monomers from isolated lignins. J. Agric. Food Chem. **46:** 547–552.

Maeda, K., Kimura, S., Demura, T., Takeda, J., and Ozeki, Y. (2005). DcMYB1 acts as a transcriptional activator of the carrot phenylalanine ammonia-lyase gene (DcPAL1) in response to elicitor treatment, UV-B irradiation and the dilution effect. Plant Mol. Biol. **59:** 739–752.

McCarthy, R.L., Zhong, R., and Ye, Z.H. (2009). MYB83 is a direct target of SND1 and acts redundantly with MYB46 in the regulation of secondary cell wall biosynthesis in Arabidopsis. Plant Cell Physiol. **50:** 1950–1964.

McNellis, T.W., Mudgett, M.B., Li, K., Aoyama, T., Horvath, D., Chua, N.H., and Staskawicz, B.J. (1998). Glucocorticoid-inducible expression of a bacterial avirulence gene in transgenic *Arabidopsis* induces hypersensitive cell death. Plant J. **14:** 247–257.

Menden, B., Kohlhoff, M., and Moerschbacher, B.M. (2007). Wheat cells accumulate a syringyl-rich lignin during the hypersensitive resistance response. Phytochemistry **68:** 513–520.

Meyer, K., Shirley, A.M., Cusumano, J.C., Bell-Lelong, D.A., and Chapple, C. (1998). Lignin monomer composition is determined by the expression of a cytochrome P450-dependent monooxygenase in Arabidopsis. Proc. Natl. Acad. Sci. USA **95:** 6619–6623.

Moerschbacher, B.M., Noll, U., Gorrichon, L., and Reisener, H.J. (1990). Specific inhibition of lignification breaks hypersensitive resistance of wheat to stem rust. Plant Physiol. **93:** 465–470.

Moreira-Vilar, F.C., Siqueira-Soares, R.C., Finger-Teixeira, A., de Oliveira, D.M., Ferro, A.P., da Rocha, G.J., Ferrarese, M.L., dos Santos, W.D., and Ferrarese-Filho, O. (2014). The acetyl bromide method is faster, simpler and presents best recovery of lignin in different herbaceous tissues than Klason and thioglycolic acid methods. PLoS One **9:** e110000.

Murashige, T., and Skoog, F. (1962). A revised medium for rapid growth and bioassays with tobacco tissue cultures. Physiol. Plant. **15:** 473–497.

Muroi, A., Ishihara, A., Tanaka, C., Ishizuka, A., Takabayashi, J., Miyoshi, H., and Nishioka, T. (2009). Accumulation of hydroxycinnamic acid amides induced by pathogen infection and identification of agmatine coumaroyltransferase in *Arabidopsis thaliana.* Planta **230:** 517–527.

Newman, L.J., Perazza, D.E., Juda, L., and Campbell, M.M. (2004). Involvement of the R2R3-MYB, AtMYB61, in the ectopic lignification and dark-photomorphogenic components of the *det3* mutant phenotype. Plant J. **37:** 239–250.

Nicholson, R.L., and Hammerschmidt, R. (1992). Phenolic compounds and their role in disease resistance. Annu. Rev. Phytopathol. **30:** 369–389.

Novaes, E., Kirst, M., Chiang, V., Winter-Sederoff, H., and Sederoff, R. (2010). Lignin and biomass: a negative correlation for wood formation and lignin content in trees. Plant Physiol. **154:** 555–561.

O'Connell, A., Holt, K., Piquemal, J., Grima-Pettenati, J., Boudet, A., Pollet, B., Lapierre, C., Petit-Conil, M., Schuch, W., and Halpin, C. (2002). Improved paper pulp from plants with suppressed cinnamoyl-CoA reductase or cinnamyl alcohol dehydrogenase. Transgenic Res. **11:** 495–503.

Öhman, D., Demedts, B., Kumar, M., Gerber, L., Gorzsás, A., Goeminne, G., Hedenström, M., Ellis, B., Boerjan, W., and Sundberg, B. (2013). MYB103 is required for *FERULATE-5-HYDROXYLASE* expression and syringyl lignin biosynthesis in Arabidopsis stems. Plant J. **73:** 63–76.

Ono, E., Wong, H.L., Kawasaki, T., Hasegawa, M., Kodama, O., and Shimamoto, K. (2001). Essential role of the small GTPase Rac in disease resistance of rice. Proc. Natl. Acad. Sci. USA **98:** 759–764.

Pallas, J.A., Paiva, N.L., Lamb, C., and Dixon, R.A. (1996). Tobacco plants epigenetically suppressed in phenylalanine ammonia-lyase expression do not develop systemic acquired resistance in response to infection by tobacco mosaic virus. Plant J. **10:** 281–293.

Pfaffl, M.W. (2001). A new mathematical model for relative quantification in real-time RT-PCR. Nucleic Acids Res. **29:** e45.

Piquemal, J., Lapierre, C., Myton, K., O'Connell, A., Schuch, W., Grima-Pettenati, J., and Boudet, A.M. (1998). Down-regulation of cinnamoyl-CoA reductase induces significant changes of lignin profiles in transgenic tobacco plants. Plant J. **13:** 71–83.

Pinçon, G., Maury, S., Hoffmann, L., Geoffroy, P., Lapierre, C., Pollet, B., and Legrand, M. (2001). Repression of O-methyltransferase genes in transgenic tobacco affects lignin synthesis and plant growth. Phytochemistry **57:** 1167–1176.

Quentin, M., et al. (2009). Imbalanced lignin biosynthesis promotes the sexual reproduction of homothallic oomycete pathogens. PLoS Pathog. **5:** e1000264.

Raes, J., Rohde, A., Christensen, J.H., Van de Peer, Y., and Boerjan, W. (2003). Genome-wide characterization of the lignification toolbox in Arabidopsis. Plant Physiol. **133:** 1051–1071.

Rivas-San Vicente, M., and Plasencia, J. (2011). Salicylic acid beyond defence: its role in plant growth and development. J. Exp. Bot. **62:** 3321–3338.

Rajniak, J., Barco, B., Clay, N.K., and Sattely, E.S. (2015). A new cyanogenic metabolite in *Arabidopsis* required for inducible pathogen defence. Nature **525:** 376–379.

Raven, J.A. (1984). Physiological correlates of the morphology of early vascular plants. Bot. J. Linn. Soc. **88:** 105–126.

Reddy, M.S., Chen, F., Shadle, G., Jackson, L., Aljoe, H., and Dixon, R.A. (2005). Targeted down-regulation of cytochrome P450 enzymes for forage quality improvement in alfalfa (*Medicago sativa* L.). Proc. Natl. Acad. Sci. USA **102:** 16573–16578.

Ride, J.P. (1975). Lignification in wounded wheat leaves in response to fungi and its possible role in resistance. Physiol. Plant Pathol. **5:** 125–134.

Robertsen, B. (1986). Elicitors of the production of lignin-like compounds in cucumber hypocotyls. Physiol. Mol. Plant Pathol. **28:** 137–148.

Robertsen, B., and Svalheim, I. (1990). The nature of lignin-like compounds in cucumber hypocotyls induced by alpha-1,4-linked oligogalacturonides. Physiol. Plant. **79:** 512–518.

Roccaro, M., and Somssich, I.E. (2011). Chromatin immunoprecipitation to identify global targets of WRKY transcription factor family members involved in plant immunity. Methods Mol. Biol. **712:** 45–58.

Rohde, A., et al. (2004). Molecular phenotyping of the *pal1* and *pal2* mutants of *Arabidopsis thaliana* reveals far-reaching consequences on phenylpropanoid, amino acid, and carbohydrate metabolism. Plant Cell **16:** 2749–2771.

Romero, I., Fuertes, A., Benito, M.J., Malpica, J.M., Leyva, A., and Paz-Ares, J. (1998). More than 80*R2R3-MYB* regulatory genes in the genome of *Arabidopsis thaliana.* Plant J. **14:** 273–284.

Sattler, S.E., Funnell-Harris, D.L., and Pedersen, J.F. (2010). Brown midrib mutations and their importance to the utilization of maize, sorghum, and pearl millet lignocellulosic tissues. Plant Sci. **178:** 229–239.

Schenke, D., Böttcher, C., and Scheel, D. (2011). Crosstalk between abiotic ultraviolet-B stress and biotic (flg22) stress signalling in Arabidopsis prevents flavonol accumulation in favor of pathogen defence compound production. Plant Cell Environ. **34:** 1849–1864.

Scully, E.D., et al. (2016). Overexpression of *SbMyb60* impacts phenylpropanoid biosynthesis and alters secondary cell wall composition in *Sorghum bicolor.* Plant J. **85:** 378–395.

Shelton, D., Stranne, M., Mikkelsen, L., Pakseresht, N., Welham, T., Hiraka, H., Tabata, S., Sato, S., Paquette, S., Wang, T.L., Martin, C., and Bailey, P. (2012). Transcription factors of Lotus: regulation of isoflavonoid biosynthesis requires coordinated changes in transcription factor activity. Plant Physiol. **159:** 531–547.

Shen, H., et al. (2013). A genomics approach to deciphering lignin biosynthesis in switchgrass. Plant Cell **25:** 4342–4361.

Shuford, C.M., Li, Q., Sun, Y.H., Chen, H.C., Wang, J., Shi, R., Sederoff, R.R., Chiang, V.L., and Muddiman, D.C. (2012). Comprehensive quantification of monolignol-pathway enzymes in *Populus trichocarpa* by protein cleavage isotope dilution mass spectrometry. J. Proteome Res. **11:** 3390–3404.

Siegrist, J., Jeblick, W., and Kauss, H. (1994). Defense responses in infected and elicited cucumber (*Cucumis sativus* L.) hypocotyl segments exhibiting acquired resistance. Plant Physiol. **105:** 1365–1374.

Siwinska, J., Kadzinski, L., Banasiuk, R., Gwizdek-Wisniewska, A., Olry, A., Banecki, B., Lojkowska, E., and Ihnatowicz, A. (2014). Identification of QTLs affecting scopolin and scopoletin biosynthesis in *Arabidopsis thaliana.* BMC Plant Biol. **14:** 280.

Smit, F., and Dubery, I.A. (1997). Cell wall reinforcement in cotton hypocotyls in response to a *Verticillium dahliae* elicitor. Phytochemistry **44:** 811–815.

Sun, H., Wang, L., Zhang, B., Ma, J., Hettenhausen, C., Cao, G., Sun, G., Wu, J., and Wu, J. (2014). Scopoletin is a phytoalexin against *Alternaria alternata* in wild tobacco dependent on jasmonate signalling. J. Exp. Bot. **65:** 4305–4315.

Sticher, L., Mauch-Mani, B., and Métraux, J.P. (1997). Systemic acquired resistance. Annu. Rev. Phytopathol. **35:** 235–270.

Stracke, R., Werber, M., and Weisshaar, B. (2001). The R2R3-MYB gene family in *Arabidopsis thaliana.* Curr. Opin. Plant Biol. **4:** 447–456.

Sugimoto, K., Takeda, S., and Hirochika, H. (2000). MYB-related transcription factor NtMYB2 induced by wounding and elicitors is a regulator of the tobacco retrotransposon Tto1 and defense-related genes. Plant Cell **12:** 2511–2528.

Thomma, B.P., Nelissen, I., Eggermont, K., and Broekaert, W.F. (1999). Deficiency in phytoalexin production causes enhanced susceptibility of *Arabidopsis thaliana* to the fungus *Alternaria brassicicola.* Plant J. **19:** 163–171.

Van Acker, R., Vanholme, R., Storme, V., Mortimer, J.C., Dupree, P., and Boerjan, W. (2013). Lignin biosynthesis perturbations affect secondary cell wall composition and saccharification yield in *Arabidopsis thaliana.* Biotechnol. Biofuels **6:** 46.

Vance, C.P. (1980). Lignification as a mechanism in disease resistance. Annu. Rev. Phytopathol. **18:** 259–288.

VanEtten, H.D., Mansfield, J.W., Bailey, J.A., and Farmer, E.E. (1994). Two classes of plant antibiotics: phytoalexins versus "phytoanticipins.". Plant Cell **6:** 1191–1192.

Vanholme, R., Demedts, B., Morreel, K., Ralph, J., and Boerjan, W. (2010). Lignin biosynthesis and structure. Plant Physiol. **153:** 895–905.

Vanholme, R., Storme, V., Vanholme, B., Sundin, L., Christensen, J.H., Goeminne, G., Halpin, C., Rohde, A., Morreel, K., and Boerjan, W. (2012). A systems biology view of responses to lignin biosynthesis perturbations in *Arabidopsis.* Plant Cell **24:** 3506–3529.

Vanholme, R., et al. (2013). Caffeoyl shikimate esterase (CSE) is an enzyme in the lignin biosynthetic pathway in *Arabidopsis.* Science **341:** 1103–1106.

Vargas, L., Cesarino, I., Vanholme, R., Voorend, W., de Lyra Soriano Saleme, M., Morreel, K., and Boerjan, W. (2016). Improving total saccharification yield of *Arabidopsis* plants by vessel-specific complementation of *caffeoyl shikimate esterase* (*cse*) mutants. Biotechnol. Biofuels **9:** 139.

Weng, J.-K., and Chapple, C. (2010). The origin and evolution of lignin biosynthesis. New Phytol. **187:** 273–285.

Xu, Q., Yin, X.R., Zeng, J.K., Ge, H., Song, M., Xu, C.J., Li, X., Ferguson, I.B., and Chen, K.S. (2014). Activator- and repressor-type MYB transcription factors are involved in chilling injury induced flesh lignification in loquat via their interactions with the phenylpropanoid pathway. J. Exp. Bot. **65:** 4349–4359.

Yanhui, C., et al. (2006). The MYB transcription factor superfamily of Arabidopsis: expression analysis and phylogenetic comparison with the rice MYB family. Plant Mol. Biol. **60:** 107–124.

Yelle, D.J., Ralph, J., and Frihart, C.R. (2008). Characterization of nonderivatized plant cell walls using high-resolution solution-state NMR spectroscopy. Magn. Reson. Chem. **46:** 508–517.

Zhong, R., Richardson, E.A., and Ye, Z.-H. (2007). The MYB46 transcription factor is a direct target of SND1 and regulates secondary wall biosynthesis in Arabidopsis. Plant Cell **19:** 2776–2792.

Zhong, R., Lee, C., Zhou, J., McCarthy, R.L., and Ye, Z.-H. (2008). A battery of transcription factors involved in the regulation of secondary cell wall biosynthesis in Arabidopsis. Plant Cell **20:** 2763–2782.

Zhong, R., and Ye, Z.-H. (2009). Transcriptional regulation of lignin biosynthesis. Plant Signal. Behav. **4:** 1028–1034.

Zhong, R., and Ye, Z.-H. (2012). MYB46 and MYB83 bind to the SMRE sites and directly activate a suite of transcription factors and secondary wall biosynthetic genes. Plant Cell Physiol. **53:** 368–380.

Zhou, J., Lee, C., Zhong, R., and Ye, Z.H. (2009). MYB58 and MYB63 are transcriptional activators of the lignin biosynthetic pathway during secondary cell wall formation in *Arabidopsis.* Plant Cell **21:** 248–266.

Zhou, R., Jackson, L., Shadle, G., Nakashima, J., Temple, S., Chen, F., and Dixon, R.A. (2010). Distinct cinnamoyl CoA reductases involved in parallel routes to lignin in *Medicago truncatula.* Proc. Natl. Acad. Sci. USA **107:** 17803–17808.

Zipfel, C. (2014). Plant pattern-recognition receptors. Trends Immunol. **35:** 345–351.

Zipfel, C., Kunze, G., Chinchilla, D., Caniard, A., Jones, J.D.G., Boller, T., and Felix, G. (2006). Perception of the bacterial PAMP EF-Tu by the receptor EFR restricts *Agrobacterium*-mediated transformation. Cell **125:** 749–760.